ESAIM: Control, Optimisation and Calculus of Variations Will be set by the publisher
URL: http://www.emath.fr/cocv/

GEOMETRIC AND NUMERICAL METHODS FOR A STATE CONSTRAINED MINIMUM TIME CONTROL PROBLEM OF AN ELECTRIC VEHICLE

Olivier Cots[1]

Abstract. In this article, the minimum time control problem of an electric vehicle is modeled as a Mayer problem in optimal control, with affine dynamics with respect to the control and with state constraints. The candidates as minimizers are selected among a set of extremals, solutions of a Hamiltonian system given by the maximum principle. An analysis, with the techniques of geometric control, is used first to reduce the set of candidates and then to construct the numerical methods. This leads to a numerical investigation based on indirect methods using the `HamPath` software. Multiple shooting and homotopy techniques are used to build a synthesis with respect to the bounds of the boundary sets.

AMS Subject Classification. 49K15, 49M05, 90C90, 80M50.

November 16, 2016.

Introduction

In this article, we are interested in the optimal control of an electric car, with a hybrid motor which can be operated in two discrete modes, $u(t) \in \{-1, 1\}$, leading either to acceleration with energy consumption, or to a breaking-induced recharging of the battery. This vehicle can be seen as a specific type of hybrid electric vehicle (HEV), which is a vast field of research. Some recent works on controlling HEVs and further references can be found in [19, 28]. Moreover, the particular model we are interested in, see equations (1), have already been studied from the optimal control point of view. In recent papers [24, 26], F. Messine *et al.* solved the problem of the minimization of the energy consumption of an electric vehicle described by equations (1) during its displacement. In this article, we intend to analyze a complementary optimal control problem by a different approach, combining geometric control and numerical methods based on the maximum principle. Besides, as mentioned in [26], optimization of driving strategy and optimization-driven assistant systems are on the rise from these last few decades, especially because of recent technological advances and successfully operating autonomous cars. One can found recent works, using different numerical approaches, such as indirect methods for off-line optimization in [20], or nonlinear model predictive control for real-time optimization in [21].

The dynamics of the electric vehicle is described with three differential states: the electric current i (in ampere), the position of the car α (in meter) and the angular velocity ω (in radian per second). The dynamical

Keywords and phrases: Geometric optimal control; state constraints; shooting and homotopy methods; electric car.

[1] Toulouse Univ., INP-ENSEEIHT-IRIT, UMR CNRS 5505, 2 rue Camichel, 31071 Toulouse, France; olivier.cots@enseeiht.fr

system is the following:

$$\begin{aligned}\frac{\mathrm{d}i}{\mathrm{d}t}(t) &= \frac{1}{L_m}\big(-R_m\, i(t) - K_m\, \omega(t) + V_{\text{alim}}\, u(t)\big)\\ \frac{\mathrm{d}\alpha}{\mathrm{d}t}(t) &= \frac{r}{K_r}\,\omega(t)\\ \frac{\mathrm{d}\omega}{\mathrm{d}t}(t) &= -\frac{K_r}{r}\, g\, K_f + \frac{K_r^2 K_m}{r^2 M}\, i(t) - \frac{1}{2}\,\rho S C_x\, \frac{r}{K_r M}\,|\omega(t)|\,\omega(t).\end{aligned} \tag{1}$$

To prevent the motor from mechanical damages, the current is bounded by $|i(t)| \leq i_{\max}$, $i_{\max} > 0$. The convexification of the control domain leads to consider the control in the whole interval $[-1\,,1]$. This convexification is justified by the fact that the motor can switch from one discrete mode to another at extremely high frequency. We may also fix some constraints on the maximal speed (*i.e.* linear velocity) of the car. The linear velocity (in km/h) is given by the relation $v(t) = \omega(t) \times 3.6\, r/K_r$ and we bound it by $|v(t)| \leq v_{\max}$, $v_{\max} > 0$. For given boundary conditions in the state space, the problem of interest is the minimization of the transfer time. Note that we consider only positive angular velocity so we replace $|\omega(t)|$ by $\omega(t)$ in the dynamics. The parameters, given in Table 1, correspond to an electric solar car.

Parameter	Description	Unit	Parameter	Description	Unit
C_x	Aerodynamic coefficient		R_m	Inductor resistance	ohms
ρ	Air density	kg/m^3	K_m	Motor torque coefficient	
V_{alim}	Battery voltage	volt	r	Radius of the wheels	m
K_f	Friction coefficient		K_r	Reduction coefficient	
	(of the wheels on the road)		R_{bat}	Resistance of the battery	ohms
g	Gravity constant	m.s^{-2}	S	Surface in front of the vehicle	m^2
L_m	Inductance of the rotor	henry	M	Total mass	kg

TABLE 1. Description of the electric solar car parameters.

Let denote by $q \coloneqq (i, \alpha, \omega)$ the state, $M \coloneqq \mathbb{R}^3$ the state space, $q_0 \in M$ the initial point, M_c a submanifold of M with boundary, M_f the terminal submanifold and $U \coloneqq [-1\,,1]$ the control domain. The optimal control problem with control and state constraints is of the form:

$$\min_{u(\cdot),\, t_f} t_f, \quad \dot{q}(t) = f(q(t), u(t)) = f_0(q(t)) + u(t)\, f_1(q(t)), \quad t \in [0\,, t_f], \quad u(t) \in U, \quad q(t) \in M_c \subset M, \quad t_f > 0,$$

with boundary conditions $q(0) = q_0 \in M$ and $q(t_f) \in M_f \subset M$. The optimal solution can be found as an extremal solution of the maximum principle (with state constraints) and analyzed with the recent advanced techniques of geometric optimal control. The in-depth analysis of the minimum time problem without state constraints leads to the conclusion that the optimal policy is a single positive bang arc, therefore the optimal control is constant and maximum everywhere. There are no subarcs with intermediate values on the norm of the control, namely singular arcs. If we take into account the state constraints, then it introduces more complex structures with boundary ($q(t) \in \partial M_c$) and interior ($q(t) \in \mathring{M}_c$) arcs. We fully determine each type of extremals and we give new junction conditions between bang and boundary arcs. Besides, the local classification of the bang-bang extremals near the switching surface combined with the analysis of the state constrained problem provides a local time minimal synthesis which gives better insight into the structure of the optimal solutions. These theoretical results are first used to reduce the set of candidates as minimizers, but they

are also necessary to build up the numerical methods. This geometric analysis leads to a numerical investigation based on indirect methods using the `HamPath` software. For one particular optimal control problem, we have to define the associated Multi-Point Boundary Value Problem which is solved by shooting techniques. However, we are interested in solving a family of optimal control problems and thus, we use differential path following (or homotopy) methods. We combine multiple shooting and homotopy techniques to study first a practical case ($i_{\max} = 150$) and then to build a synthesis with respect to the parameters $i_{\max}$ and $v_{\max}$.

The paper is organized as follows. The optimal control problem is defined in section 1. In section 2, we analyze the state unconstrained problem, while section 3 is devoted to the state constrained case. The numerical methods are presented in section 4 and section 5 describes the numerical simulations. Section 6 concludes the article.

1. The Mathematical model and the Mayer optimal control problem

1.1. **Preliminaries**

We first recall some basic facts from symplectic and differential geometries to introduce the Hamiltonian function and the adjoint vector (or covector). Most of the notations are taken from [1].

Let M be a smooth manifold of dimension n. Let T^*M denote the cotangent bundle of M and σ the canonical symplectic form on T^*M. Recall that (T^*M, σ) is a *symplectic manifold*, that is, σ is a smooth exterior 2-form on T^*M which is closed and non-degenerated. For a smooth function h on T^*M, we write $\vec{h}$ the *Hamiltonian vector field* on T^*M defined by $i_{\vec{h}}\sigma = -\,\mathrm{d}h$, where $i_{\vec{h}}\sigma$ is the interior product of σ by $\vec{h}$: $\forall\, z \in T^*M$, $\forall\, w \in T_z(T^*M)$, $i_{\vec{h}}\sigma_z \cdot w \coloneqq \sigma_z(\vec{h}(z), w)$. The function h is called the *Hamiltonian* function.

Let (q, p) denote the Darboux coordinates on T^*M. In these canonical coordinates, the Liouville 1-form $s \in \Lambda^1(T^*M)$ writes $s = p\,\mathrm{d}q$, and the canonical symplectic form is $\sigma = \mathrm{d}s = \mathrm{d}p \wedge \mathrm{d}q$. If $\varphi\colon M \to N$ is a smooth mapping between smooth manifolds, then its differential $\varphi_*\colon T_qM \to T_xN$, $q \in M$, $x = \varphi(q)$, has an adjoint mapping $\varphi^* \coloneqq (\varphi_*)^*\colon T^*_xN \to T^*_qM$ defined as follows: $\forall\, p_x \in T^*_xN$, $\varphi^* p_x = p_x \circ \varphi_*$, and $\forall\, v \in T_qM$, $\langle \varphi^* p_x, v\rangle = \langle p_x, \varphi_* v\rangle$. If φ is a diffeomorphism on M, then it induces the lifted diffeomorphism Φ on T^*M, $\Phi(p, q) \coloneqq (\varphi(q), (\varphi^*)^{-1}p)$, which is a Mathieu symplectic transformation.

Notation

Here, we adopt the following notation used throughout the paper. Let F_0, F_1 be two smooth vector fields on M, c a smooth function on M. We use $\mathrm{ad}\, F_0$ to denote the operator acting on vector fields $F_1 \mapsto [F_0, F_1] \coloneqq F_0 \cdot F_1 - F_1 \cdot F_0$, with $(F_0 \cdot F_1)(x) = \mathrm{d}F_1(x)\, F_0(x)$, which gives the *Lie bracket*. The *Lie derivative* $\mathcal{L}_{F_0} c$ of c along F_0 is simply written $F_0 \cdot c$. Denoting H_0, H_1 the Hamiltonian lifts of F_0, F_1, then the *Poisson bracket* of H_0 and H_1 is $\{H_0, H_1\} \coloneqq \overrightarrow{H_0} \cdot H_1$. We also use the notation H_{01} (resp. F_{01}) to write the bracket $\{H_0, H_1\}$ (resp. $[F_0, F_1]$) and so forth. Besides, since H_0, H_1 are Hamiltonian lifts, we have $\{H_0, H_1\} = \langle p, [F_0, F_1]\rangle$.

1.2. **Electric car model**

The dynamics of the electric car is given by the smooth control vector field: $(q, u) \in M \times U \to f(q, u) \in T_qM$. We make a simple normalization introducing the diffeomorphism on M,

$$x \coloneqq \varphi(q) = \left(\frac{q_1}{i_{\max}}, \frac{q_2}{\alpha_f}, \frac{q_3}{\omega_{\max}}\right), \quad q = (q_1, q_2, q_3),$$

where $i_{\max} > 0$ is the maximal current, $\alpha_f > 0$ is the wished final position (*i.e.* the position to reach at final time) and $w_{\max} > 0$ is the maximal angular velocity. We define also $v_{\max} \coloneqq w_{\max} \times 3.6\, r/K_r$ the maximal linear velocity. The dynamics becomes:

$$\dot{x}(t) = \mathrm{d}\varphi(\varphi^{-1}(x(t))) \cdot f(\varphi^{-1}(x(t)), u(t)) \coloneqq F(x(t), u(t)),$$

and any covector $p \in T^*_qM$ is transformed to the covector p_x, with the relation $p = {}^t\,\mathrm{d}\varphi(\varphi^{-1}(x))\, p_x$.

Remark 1.1. From now on, we denote by p the covector p_x to simplify notations.

We introduce the vector of parameters

$$w \coloneqq \left(\frac{1}{L_m}, R_m, K_m, V_{\text{alim}}, \frac{r}{K_r}, g\,K_f, \frac{1}{M}, \frac{1}{2}\rho\,S\,C_x, R_{\text{bat}}, i_{\max}, \alpha_f, \omega_{\max}\right),$$

and we have $\forall i \in [\![1, 12]\!]$, $w_i > 0$. In the x-coordinates, the dynamics writes

$$\dot{x}(t) = F_0(x(t)) + u(t)\,F_1(x(t)), \quad x(t) \in \mathbb{R}^3, \tag{2}$$

where the smooth vector fields are given by

$$F_0(x) = (a_1x_1 + a_2x_3)\frac{\partial}{\partial x_1} + a_3x_3\frac{\partial}{\partial x_2} + (a_4 + a_5x_1 + a_6x_3^2)\frac{\partial}{\partial x_3}, \quad F_1(x) = a_7\frac{\partial}{\partial x_1},$$

with

$$\begin{aligned} &a_1 = -w_1w_2, \quad a_2 = -\frac{w_1w_3w_{12}}{w_{10}}, \quad a_3 = \frac{w_5w_{12}}{w_{11}}, \\ &a_4 = -\frac{w_6}{w_5w_{12}}, \quad a_5 = \frac{w_3w_7w_{10}}{w_5^2w_{12}}, \quad a_6 = -w_5w_7w_8w_{12}, \quad a_7 = \frac{w_1w_4}{w_{10}}. \end{aligned}$$

Definition 1.2. *The minimum time control problem of the electric vehicle* is the following optimal control problem (P_{tmin}): starting from $x_0 = (0, 0, 0)$, reach in the minimum time t_f the fixed normalized position $x_2(t_f) = 1$ (corresponding to $q_2(t_f) = \alpha_f$), while satisfying the following control and path constraints:

$$\begin{aligned} &u(t) \in U \coloneqq [-1\,, 1], \quad t \in [0\,, t_f] \text{ a.e.}, \\ &x(t) \in M_c \coloneqq [-1\,, 1] \times \mathbb{R} \times [-1\,, 1] \subset M \coloneqq \mathbb{R}^3, \quad t \in [0\,, t_f]. \end{aligned}$$

In this article we are interested in solving (P_{tmin}) for different values of $w_{10} = i_{\max}$ and $w_{12} = \omega_{\max}$. The problem (P_{tmin}) can be stated as a *Mayer problem* summerized this way:

$$\left\{\begin{array}{ll} g(t_f, x(t_f)) & \coloneqq t_f \longrightarrow \min\limits_{u(\cdot),\, t_f}, \\ \dot{x}(t) & = F_0(x(t)) + u(t)\,F_1(x(t)), \quad u(t) \in U, \quad t \in [0\,, t_f] \text{ a.e.}, \quad t_f > 0, \\ x(0) & = x_0, \\ x(t) & \in M_c, \quad t \in [0\,, t_f], \\ b(x(t_f)) & \coloneqq x_2(t_f) - 1 = 0. \end{array}\right. \tag{P_{tmin}}$$

Remark 1.3. In [24, 26], the authors investigate the problem of the minimization of the energy consumption, the transfer time t_f being fixed. It is then reasonable to study the minimum time problem. The energy minimum problem can be stated as a Mayer problem of the following form:

$$\left\{\begin{array}{ll} g(t_f, \widetilde{x}(t_f)) & \coloneqq x_4(t_f) \longrightarrow \min\limits_{u(\cdot)}, \quad \widetilde{x} \coloneqq (x, x_4) \in \mathbb{R}^4, \quad t_f \text{ fixed}, \\ \dot{\widetilde{x}}(t) & = \widetilde{F}_0(\widetilde{x}(t)) + u(t)\,\widetilde{F}_1(\widetilde{x}(t)), \quad u(t) \in U, \quad t \in [0\,, t_f] \text{ a.e.}, \\ x(0) & = x_0, \quad x_4(0) = 0, \\ x(t) & \in M_c, \quad t \in [0\,, t_f], \\ b(x(t_f)) & = 0, \end{array}\right. \tag{P_{emin}}$$

where $\widetilde{F}_0(\widetilde{x}) \coloneqq F_0(x) + w_9w_{10}^2x_1^2\dfrac{\partial}{\partial x_4}$ and $\widetilde{F}_1(\widetilde{x}) \coloneqq F_1(x) + w_4w_{10}x_1\dfrac{\partial}{\partial x_4}$.

2. Geometric analysis of problem (P_{tmin}) without state constraints

2.1. Necessary optimality conditions

Let consider the problem (P_{tmin}) and assume the state constraints are relaxed: $M_c = M$. This optimal control problem can be written as the infinite dimensional minimization problem:

$$\min\{t_f \mid t_f > 0,\, u(\cdot) \in \mathcal{U},\, b \circ E_{x_0}(t_f, u(\cdot)) = 0\},$$

where $x_0 \in M$ is fixed, $\mathcal{U} \coloneqq \mathrm{L}^\infty([0\,, t_f], U)$ is the set of *admissible controls*[1], and where E_{x_0} is the *end-point mapping* defined by: $E_{x_0} \colon \mathbb{R}^+ \times \mathcal{U} \to M$, $E_{x_0}(t, u(\cdot)) \coloneqq x(t, x_0, u(\cdot))$, where $t \mapsto x(t, x_0, u(\cdot))$ is the trajectory solution of (2), corresponding to the control $u(\cdot)$ such that $x(0, x_0, u(\cdot)) = x_0$.

This leads to the following necessary optimality conditions according to the Pontryagin Maximum Principle (PMP), see [3]. Define the pseudo-Hamiltonian:

$$\begin{array}{rcl} H \colon T^*M \times U & \longrightarrow & \mathbb{R} \\ (x, p, u) & \longmapsto & H(x, p, u) \coloneqq \langle p, F_0(x) + u\, F_1(x) \rangle\,. \end{array}$$

By virtue of the *maximum principle*, if $(\bar u(\cdot), \bar t_f)$ is optimal then the associated trajectory $\bar x(\cdot)$ is the projection of an absolutely continuous integral curve $(\bar x(\cdot), \bar p(\cdot)) \colon [0\,, \bar t_f] \to T^*M$ of $\overrightarrow{H} \coloneqq (\frac{\partial H}{\partial p}, -\frac{\partial H}{\partial x})$ such that the following *maximization condition* holds for almost every $t \in [0\,, \bar t_f]$:

$$H(\bar x(t), \bar p(t), \bar u(t)) = \max_{u \in U} H(\bar x(t), \bar p(t), u). \tag{3}$$

Note that the function $h(\bar x(t), \bar p(t)) \coloneqq H(\bar x(t), \bar p(t), \bar u(t))$ is constant. The boundary conditions must be satisfied and we have the following *transversality conditions*:

$$\bar p(\bar t_f) = \mu\, b'(\bar x(\bar t_f)) = (0, \mu, 0), \quad \mu \in \mathbb{R}.$$

Since t_f is free, if $\bar u(\cdot)$ is continuous at time $\bar t_f$, then

$$H(\bar x(\bar t_f), \bar p(\bar t_f), \bar u(\bar t_f)) = -p^0\, \frac{\partial g}{\partial t}(\bar t_f, \bar x(\bar t_f)) = -p^0, \quad p^0 \in \mathbb{R}. \tag{4}$$

Moreover, the constant p^0 is nonpositive and $(\bar p(\cdot), p^0) \neq (0, 0)$. Either $p^0 = 0$ (*abnormal case*), or p^0 can be set to -1 by homogeneity (*normal case*). Since x_2 is cyclic, p_2 defines a first integral and the translation $x_2 \to x_2 + c$ defines a one-parameter group of symmetries. This is due to Noether theorem in Hamiltonian form. Hence, by symmetry, we can fix $x_2(0) = 0$. The adjoint equation is

$$\dot p(t) = -p(t)\, F_0'(x(t)) = -\left(a_1 p_1(t) + a_5 p_3(t)\right) \frac{\partial}{\partial p_1} - \left(a_2 p_1(t) + a_3 p_2 + 2 a_6 x_3(t) p_3(t)\right) \frac{\partial}{\partial p_3}.$$

Note that h defines a second first integral and that $\bar p_2 = \mu \neq 0$, otherwise we would have $\bar p(\bar t_f) = 0$ which would imply $h(\bar x(t), \bar p(t)) = -p^0 = 0$, and $(\bar p(\bar t_f), p^0) = (0, 0)$ is not possible.

Proposition 2.1. *$p^0 = 0$ (abnormal case) if and only if $\bar x_3(\bar t_f) = 0$.*

Proof. We have $H(\bar x(\bar t_f), \bar p(\bar t_f), \bar u(\bar t_f)) = \bar p_2 a_3 \bar x_3(\bar t_f) = -p^0$, with $\bar p_2 \neq 0$. The result follows. □

[1] The set of admissible controls is the set of L^∞-mappings on $[0\,, t_f]$ taking their values in U such that the associated trajectory $x(\cdot)$ is globally defined on $[0\,, t_f]$.

Definition 2.2. A triple $(x(\cdot), p(\cdot), u(\cdot))$ where $(x(\cdot), p(\cdot))$ is an integral curve of $\vec{H}$ and satisfying (3) is called an *extremal*. Any extremal satisfying the boundary conditions, the transversality conditions and condition (4) is called a BC-extremal. Let $(\bar{z}(\cdot), \bar{u}(\cdot))$ be an extremal, with $\bar{z}(\cdot) \coloneqq (\bar{x}(\cdot), \bar{p}(\cdot))$. If h is defined and smooth in a neighborhood of $\bar{z}$ then h defines a *true Hamiltonian*, and $\bar{z}$ is also an integral curve of $\vec{h}$. We define the *Hamiltonian lifts* $H_0(x,p) \coloneqq \langle p, F_0(x)\rangle$, $H_1(x,p) \coloneqq \langle p, F_1(x)\rangle$ and the *switching function* $\Phi(t) \coloneqq H_1(x(t), p(t))$.

Regular extremals

It follows from (3) that if $\Phi(t) \neq 0$, $u(t) = \operatorname{sign}(\Phi(t))$. We say that a trajectory $x(\cdot)$ restricted to a subinterval $I \subset [0\,, t_f]$, not reduced to a singleton, is a *bang arc* if $u(\cdot)$ is constant on I, taking values in $\{-1, 1\}$. The trajectory is called *bang-bang* if it is the concatenation of a finite number of bang arcs.

Singular extremals

We say that a trajectory $x(\cdot)$ restricted to a subinterval $I \subset [0\,, t_f]$, not reduced to a singleton, is a *singular arc* if the associated extremal lift satisfies $\Phi(t) = 0$, $\forall t \in I$. A trajectory $x(\cdot)$ defined on $[0\,, t_f]$, with $x(0) = x_0$, is singular if the associated control $u(\cdot)$ is a critical point of $u(\cdot) \mapsto E_{x_0}(u(\cdot), t_f)$. In this case, $u(\cdot)$ is said to be singular. From the geometric point of view, a control $\bar{u}(\cdot) \in \mathcal{U}$ such that $E_{x_0}(\bar{u}(\cdot), t_f) \in \partial\mathcal{A}(x_0, t_f)$, where $\mathcal{A}(x_0, t_f) \coloneqq \{E_{x_0}(u(\cdot), t_f) \mid u(\cdot) \in \mathcal{U}\}$ is the accessibility set at time t_f, is singular.

2.2. **Lie bracket configuration**

The local behavior of the affine control system (2) is determined by the values of the drift F_0, the control vector field F_1, and all their Lie brackets at a reference point $x \in M$. Loosely speaking, the values and dependencies of these vector fields at x is called the *Lie bracket configuration* of the system at x. According to [27, Chapter 7], the concept of *codimension* is crucial to organize the Lie bracket conditions into groups of increasing degrees of degeneracy. The codimension is given by the number of linearly independent "relevant" equality relations that hold between these vector fields at x. As both the dimension of the state space and the codimension of the Lie bracket configuration at the point x increase, the local optimal synthesis becomes increasingly more complex. According to the following lemma, the 3-dimensional system (2) is a part of the codimension-0 case[2].

Lemma 2.3. *We have:*

i)
$$\begin{cases} F_{01} & = -a_7\big(a_1 \frac{\partial}{\partial x_1} + a_5 \frac{\partial}{\partial x_3}\big), \\ F_{001} & = a_7\Big(\big(a_1^2 + a_2 a_5\big)\frac{\partial}{\partial x_1} + a_3 a_5 \frac{\partial}{\partial x_2} + a_5\big(a_1 + 2a_6 x_3\big)\frac{\partial}{\partial x_3}\Big), \\ F_{101} & = F_{1001} = 0, \\ F_{10001} & = 2a_5^2 a_6 a_7^2 \frac{\partial}{\partial x_3}, \end{cases}$$

ii) $\dim \operatorname{Span}(F_1(x), F_{01}(x), F_{001}(x)) = 3$ *and* $\operatorname{Lie}_x(\{F_0, F_1\}) = T_xM$, $x \in M$ *([3]).*

iii) $\dim \operatorname{Span}(F_0(x), F_1(x), F_{01}(x)) = 3$, $x \in M$, $x_3 \neq 0$.

Proof. The proof is straightforward.

i) Computing, $F_{01} = \operatorname{ad} F_0 \cdot F_1 = -F_1 \cdot F_0$ and $F_{001} = \operatorname{ad} F_0 \cdot F_{01} = -F_{01} \cdot F_0$. Computing again, $F_{101} = F_1 \cdot F_{01} - F_{01} \cdot F_1 = 0$, since F_1 and F_{01} does not depend on x. Using the *Jacobi identity*, $F_{1001} = [F_1, [F_0, F_{01}]] = -[F_0, [F_{01}, F_1]] - [F_{01}, [F_1, F_0]] = [F_0, F_{101}] + [F_{01}, F_{01}] = 0$. Computing, $F_{10001} = 2a_5^2 a_6 a_7^2 \frac{\partial}{\partial x_3}$.

ii) Let $x \in M$, then $\det(F_1(x), F_{01}(x), F_{001}(x)) = a_3 a_5^2 a_7^3 \neq 0$, so $\operatorname{Lie}_x(\{F_0, F_1\}) = T_xM$.

iii) Let $x \in M$, then $\det(F_0(x), F_1(x), F_{01}(x)) = a_3 a_5 a_7^2 x_3 \neq 0$, when $x_3 \neq 0$.

□

[2] The points such that $x_3 = 0$ have different linearly independent equality relations than the others.

[3] $\operatorname{Lie}_x(\{F_0, F_1\})$ is the Lie algebra generated by the family $\{F_0, F_1\}$ at x.

2.3. **Regular extremals**

Lemma 2.4. *The switching function* Φ *is* C^3.

Proof. $\Phi = H_1 = a_7 p_1$ is absolutely continuous, so differentiable almost everywhere. $\dot{\Phi} = H_{01} = -a_7(a_1 p_1 + a_5 p_3)$ is absolutely continuous, therefore continuous, and so Φ is C^1. Likewise $\dot{\Phi} = H_{01}$, $\ddot{\Phi} = H_{001} + u\, H_{101} = H_{001}$ (since $H_{101} = 0$ by lemma 2.3) and $\dddot{\Phi} = H_{0001} + u\, H_{1001} = H_{0001}$ (since $H_{1001} = 0$) are absolutely continuous and we can conclude that Φ is C^3. □

Proposition 2.5. *Every extremal is bang-bang.*

Proof. Let $(z(\cdot), u(\cdot))$ be an extremal defined on $[0\,, t_f]$. Let assume there exists a singular part $z_s(\cdot) = (x_s(\cdot), p_s(\cdot))$ defined on $I \subset [0\,, t_f]$. Then for all $t \in I$, $0 = \Phi(t) = H_1(z_s(t))$. Differentiating twice with respect to time, we have $0 = H_1(z_s(t)) = H_{01}(z_s(t)) = H_{001}(z_s(t))$ which implies $p_s(\cdot) = 0$ since $F_1(x_s(t))$, $F_{01}(x_s(t))$ and $F_{001}(x_s(t))$ are independent, which is not possible. □

Proposition 2.6. *The switching function has finitely many zeros.*

Proof. Following the proof of [18, proposition 2.1], if not, then along $(z(\cdot), u(\cdot))$ defined on $[0\,, t_f]$, there exists a sequence $(t_k)_k$, $t_k \in [0\,, t_f]$, all disctinct, such that $\Phi(t_k) = 0$. But t_f is fixed, so there exists a subsequence, always noted $(t_k)_k$, which converges to $\bar{t}$. As Φ is C^0, $\Phi(\bar{t}) = 0$. But Φ is also C^1, hence

$$\frac{\Phi(t_k) - \Phi(\bar{t})}{t_k - \bar{t}} = 0 \longrightarrow \dot{\Phi}(\bar{t}) = 0.$$

Besides, by Rolle's theorem, for every k, there exists at least one $\tau_k \in (t_k\,, t_{k+1})$ such that $\dot{\Phi}(\tau_k) = 0$, and by squeeze theorem the sequence $(\tau_k)_k$ converges to $\bar{t}$. But Φ is also C^2 and we have

$$\frac{\dot{\Phi}(\tau_k) - \dot{\Phi}(\bar{t})}{\tau_k - \bar{t}} = 0 \longrightarrow \ddot{\Phi}(\bar{t}) = 0.$$

In conclusion, at time $\bar{t} \in [0\,, t_f]$, $\Phi(\bar{t}) = \dot{\Phi}(\bar{t}) = \ddot{\Phi}(\bar{t}) = 0$, whence $p(\bar{t}) = 0$ which is impossible. □

Hence, any BC-extremal is a concatenation of only bang arcs. It is a difficult task to give upper bounds on the number of switchings for global time-optimal trajectories. However, any global time-optimal trajectory is locally time-optimal and next section is dedicated to the classification of such local bang-bang time-optimal trajectories.

2.4. **Classification of bang-bang extremals**

We define first the colinear set $C := \{x \in M \mid F_0(x) \parallel F_1(x)\}$. Then $x \in C$ if and only if $x_3 = 0$ and $a_4 + a_5 x_1 = 0$. The point $(x, u) = (-\frac{a_4}{a_5}, x_2, 0, \frac{a_1 a_4}{a_5 a_7})$, $x_2 \in \mathbb{R}$, is an equilibrium point of the control system (2). Let then define the following sets:

$$\Sigma_1^+ := \{z \in T^*M \mid H_1(z) > 0\}\,, \quad \Sigma_1^0 := \{z \in T^*M \mid H_1(z) = 0\}\,, \quad \Sigma_1^- := \{z \in T^*M \mid H_1(z) < 0\}\,,$$

and

$$\Sigma_{01}^+ := \{z \in T^*M \mid H_{01}(z) > 0\}\,, \quad \Sigma_{01}^0 := \{z \in T^*M \mid H_{01}(z) = 0\}\,, \quad \Sigma_{01}^- := \{z \in T^*M \mid H_{01}(z) < 0\}\,.$$

Singular extremals (if any) are entirely contained in $\Sigma_s := \Sigma_1^0 \cap \Sigma_{01}^0$. A crucial point is to apply the results obtained by Kupka [22] (see also [5]) to classify extremal curves near the *switching surface* Σ_1^0. We label γ_b a bang extremal, γ_+, γ_-, a bang extremal such that $u(\cdot) = +1$, $u(\cdot) = -1$ and γ_s a singular extremal. We denote by $\gamma_1\gamma_2$, the concatenation of an arc γ_1 followed by an arc γ_2. Since for every $z \in T^*M$, $\ker \mathrm{d}H_1(z)$ is transverse to $\ker \mathrm{d}H_{01}(z)$, then Σ_1^0 and Σ_{01}^0 are both smooth submanifold of codimension 1 transverse at each point.

2.4.1. *Normal switching points*

It is the case when a bang arc has a contact of order 1 with the switching surface. Let $\bar{z} \coloneqq (\bar{x}, \bar{p}) \in \Sigma_1^0 \setminus \Sigma_{01}^0$ and assume $\bar{x} \notin C$. The point $\bar{z}$ is called *normal*. Let $(z(\cdot), u(\cdot))$ be a regular extremal passing through $\bar{z}$ at time $\bar{t}$, then $\Phi(\bar{t}) = H_1(\bar{z}) = 0$, $\dot{\Phi}(\bar{t}) = H_{01}(\bar{z}) \neq 0$ and Φ changes its sign at $\bar{t}$. Since $\Phi(\bar{t}+s) = \dot{\Phi}(\bar{t})\, s + o(s)$ near $\bar{t}$, then locally

$$u(\bar{t}+s) = \frac{\Phi(\bar{t}+s)}{|\Phi(\bar{t}+s)|} = \frac{\dot{\Phi}(\bar{t})}{|\dot{\Phi}(\bar{t})|} \cdot \frac{s}{|s|} + o(1)\,,$$

so near $\bar{z}$, every extremal is of the form $\gamma_+\gamma_-$ if $\dot{\Phi}(\bar{t}) < 0$ and $\gamma_-\gamma_+$ if $\dot{\Phi}(\bar{t}) > 0$, see Fig. 1.

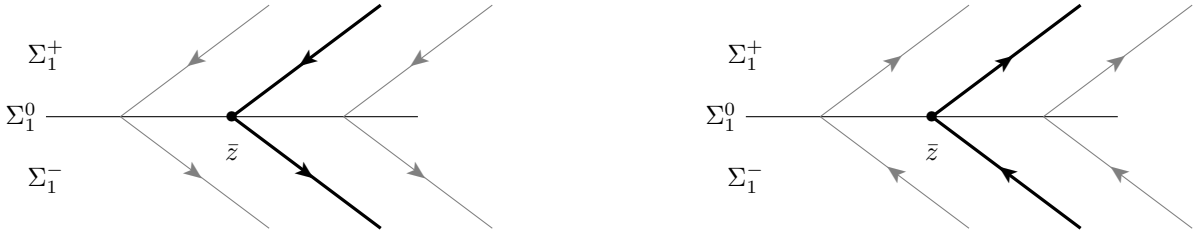

FIGURE 1. Bang-Bang extremal with contact of order 1. (Left) $\dot{\Phi}(\bar{t}) < 0$. (Right) $\dot{\Phi}(\bar{t}) > 0$.

Proposition 2.7. *Let $\bar{z} \coloneqq (\bar{x}, \bar{p}) \in T^*M$, $\bar{x} \notin C$, then $\bar{z}$ is a normal switching point if and only if $\bar{p}_1 = 0$ and $\bar{p}_3 \neq 0$. If $\bar{z}$ is a normal switching point, then locally, any extremal is of the form $\gamma_+\gamma_-$ if $\bar{p}_3 > 0$ and $\gamma_-\gamma_+$ if $\bar{p}_3 < 0$.*

2.4.2. *The fold case*

It is the case when a bang arc has a contact of order 2 with the switching surface. Let $\bar{z} \coloneqq (\bar{x}, \bar{p}) \in \Sigma_s$ and assume $\bar{x} \notin C$. We define $H_\pm \coloneqq H_0 \pm H_1$ and then we get $\Sigma_1^0 = \{z \in T^*M \mid H_+(z) - H_-(z) = 0\}$ and $\Sigma_{01}^0 = \{z \in T^*M \mid \{H_+, H_-\}(z) = 0\}$.

Lemma 2.8. *Let $(z(\cdot), u(\cdot))$ be a regular extremal passing through $\bar{z} \in \Sigma_s$ at time $\bar{t}$, then both Hamiltonian vector fields $\overrightarrow{H_+}$ and $\overrightarrow{H_-}$ are tangent to Σ_1^0 at $z(\bar{t}) = \bar{z}$.*

Proof. $\overrightarrow{H_+}(\bar{z}) \in T_{\bar{z}}\Sigma_1^0$ since $(\,\mathrm{d}H_+ - \mathrm{d}H_-) \cdot \overrightarrow{H_+} = \{H_+, H_+ - H_-\} = -\{H_+, H_-\}$ which is zero at $\bar{z}$ since $\bar{z} \in \Sigma_{01}^0$. The same result goes for $\overrightarrow{H_-}$. □

If we set $\ddot{\Phi}_\pm \coloneqq H_{001} \pm H_{101}$ then if both $\ddot{\Phi}_\pm \neq 0$, the contact of the trajectories of $\overrightarrow{H_+}$ and $\overrightarrow{H_-}$ with Σ_1^0 is of order 2. Such a point is called a *fold*. According to [22], we have three cases:

i) $\ddot{\Phi}_+\ddot{\Phi}_- > 0$: parabolic case,
ii) $\ddot{\Phi}_+ > 0$ and $\ddot{\Phi}_- < 0$: hyperbolic case,
iii) $\ddot{\Phi}_+ < 0$ and $\ddot{\Phi}_- > 0$: elliptic case.

Proposition 2.9. *The contacts with the switching surface are at most of order 2. Let $\bar{z} \coloneqq (\bar{x}, \bar{p}) \in T^*M$, $\bar{x} \notin C$, then $\bar{z}$ is a fold point if and only if $\bar{p}_1 = \bar{p}_3 = 0$ and $\bar{p}_2 \neq 0$, and if $\bar{z}$ is a fold point, it is parabolic.*

Proof. With exactly the same argument as in Proposition 2.5, contacts of order 3 or more are not possible. Let $\bar{z} \coloneqq (\bar{x}, \bar{p}) \in T^*M$, then $\bar{z}$ is a fold point iff $H_1(\bar{z}) = H_{01}(\bar{z}) = 0$ and $H_{001}(\bar{z}) \neq 0$, since $\ddot{\Phi} = H_{001}$, which gives the result. It is then a parabolic point since $\ddot{\Phi}_+ = \ddot{\Phi}_- = H_{001}$. □

We give the generic classification of extremals near a fold point only in the parabolic case. In this case, if there exists a singular extremal of minimal order passing through $\bar{z}$ (*i.e.* $H_{101}(\bar{z}) \neq 0$), this extremal is not admissible

and every extremal curve near $\bar{z}$ is bang-bang with at most two switchings, *i.e.* is of the form $\gamma_+\gamma_-\gamma_+$ or $\gamma_-\gamma_+\gamma_-$ (by convention each arc of the sequence can be empty). One extremal is time minimizing while the other is time maximizing, depending on the sign of $\ddot{\Phi}(\bar{t})$, see Fig. 2.

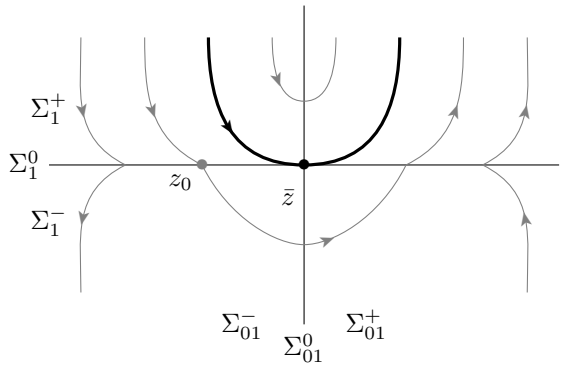

FIGURE 2. Local optimal synthesis in a neighborhood of $\bar{z}$, for $\ddot{\Phi}(\bar{t}) > 0$.

Application to problem (P_{tmin})

Let $(z(\cdot), u(\cdot))$ be a regular extremal passing through $\bar{z}$ at time $\bar{t}$, then $\Phi(\bar{t}+s) = \frac{1}{2}\ddot{\Phi}(\bar{t})\, s^2 + o\big(s^2\big)$ near $\bar{t}$, and locally,

$$u(\bar{t}+s) = \frac{\Phi(\bar{t}+s)}{|\Phi(\bar{t}+s)|} = \frac{\ddot{\Phi}(\bar{t})}{|\ddot{\Phi}(\bar{t})|} + o(1)\,.$$

Since $\bar{z}$ is a fold point, then $\ddot{\Phi}(\bar{t}) = a_3a_5a_7p_2$, with p_2 constant along any extremal and $a_3a_5a_7 > 0$. Besides, if $(z(\cdot), u(\cdot))$ is a normal BC-extremal, then according to section 2.1, $1 = h(z(t_f)) = H_0(z(t_f)) = a_3x_3(t_f)p_2$, $a_3 > 0$, and because we want to steer the vehicle from a zero position to a positive position in minimum time, $x_3(t_f)$ must be positive. As a consequence, $p_2 > 0$.

Let consider now a normal switching point z_0, close to $\bar{z}$. Let $(z(\cdot), u(\cdot))$ be an extremal of the form $\gamma_+\gamma_-\gamma_+$, γ_- non-empty, passing through z_0 at time t_0. The switching function may be approximated by

$$\Phi(t_0+s) \approx \dot{\Phi}(t_0)\, s + \frac{1}{2}\ddot{\Phi}(t_0)\, s^2,$$

with $\dot{\Phi}(t_0) < 0$ and $\ddot{\Phi}(t_0) > 0$. Hence, the switching function vanishes at t_0 and near $t_0 + s^*$, where

$$s^* = -2\frac{\dot{\Phi}(t_0)}{\ddot{\Phi}(t_0)} > 0.$$

Putting all together, we have the following proposition.

Proposition 2.10. *Let $\bar{z} \in T^*M$ be a fold point, then $H_{001}(\bar{z}) > 0$ for any normal BC-extremal passing trough $\bar{z}$ and the optimal policy near $\bar{z}$ is $\gamma_+\gamma_-\gamma_+$. Besides, the length s of γ_- is given by*

$$s \approx 2\,\frac{p_3(t_0)}{a_3p_2 + p_3(t_0)\,(a_1 + 2a_6x_3(t_0))},$$

where t_0 is the first switching time, between γ_+ and γ_-.

2.5. Optimality of the γ_+ trajectory

We conclude the section 2 showing that the strategy γ_+ is optimal. The transversality conditions imply that any BC-extremal ends at a fold point. By proposition 2.10, the last bang arc must be a positive bang. Let $\bar{t}_f \approx 5.6156$ denote the time when the γ_+ BC-extremal reaches the target $x_2 = 1$. Since the final submanifold M_f is of codimension 1 and by homogeneity, the final adjoint vector is uniquely determined for each $x_f \in M_f$. For all $x_f \in M_f$ the final adjoint vector is $p_f := (0, p_2, 0)$, with $p_2 > 0$, and we can fix $p_2 = 1$. Let $Z_f := M_f \times \{p_f\}$ and write $z(\cdot, z_f)$, $z_f \in Z_f$, the solution of H_+ starting from z_f and computed with backward integration. If for all $z_f \in Z_f$ and for all $t \in (0\,, \bar{t}_f]$, $\phi(t) = H_1(z(t, z_f)) \neq 0$, then the strategy γ_+ is optimal.

Proposition 2.11. *For the case study of problem (P_{tmin}) described in section 5.1, the strategy γ_+ is optimal.*

Proof. The final submanifold is $M_f = [-1\,, 1] \times \{1\} \times [0\,, 1]$. According to the left subgraph of Figure 3, for all $z_f \in Z_f$ and for all $t \in (0\,, \bar{t}_f]$, $\phi(t) = H_1(z(t, z_f)) \neq 0$. The values of the parameters are given in Table 3 with $\alpha_f = 100$, $i_{\max} = 1200$ and $v_{\max} = 120$. □

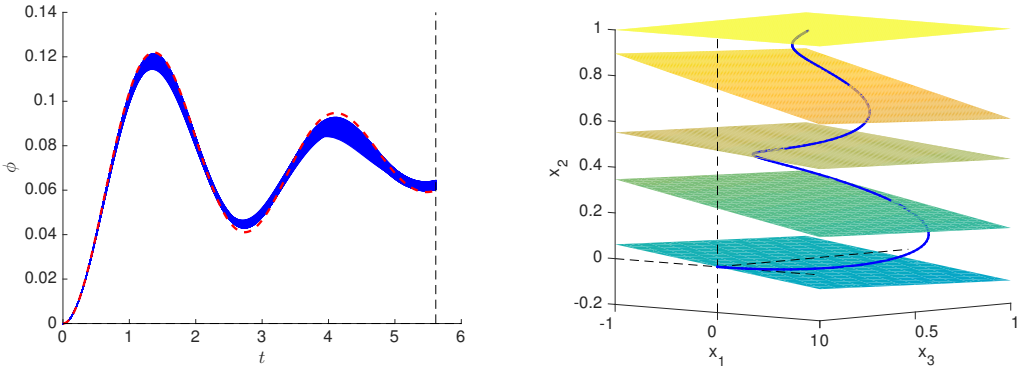

FIGURE 3. (Left) The blue plain lines represent the switching functions $\phi(t) = H_1(z(t, z_f))$, $t \in [0\,, \bar{t}_f]$, for a set of points $z_f := (x_f, p_f)$ with $x_f \in M_f$, $p_f = (0, 1, 0)$, where M_f is sampled using a fine grid, and where $z(\cdot, z_f)$ is the solution of H_+ starting from z_f computed with backward integration. The red dashed line is the switching function when the dynamics eq. (2) is linear, *i.e.* $a_6 = 0$. (Right) The evolution of M_f at times 0, $0.25\,\bar{t}_f$, $0.5\,\bar{t}_f$, $0.75\,\bar{t}_f$ and $\bar{t}_f$, by backward integration. The blue curve is the optimal γ_+ trajectory.

3. GEOMETRIC ANALYSIS OF PROBLEM (P_{tmin}) (WITH STATE CONSTRAINTS)

3.1. Abstract formulation

In this section, we consider the problem (P_{tmin}) with state constraints on x_1 and x_3, *i.e.* on the electric current and the speed of the vehicle. For both state variables x_i, $i = 1, 3$, there are two constraints: $x_i \leq 1$ and $-1 \leq x_i$ but these two constraints cannot be active at the same time, that is we cannot have $x_i(t) = 1$ and $x_i(t) = -1$ at a time t. Moreover, since x_1 and x_3 may saturate one of their constraint at the same time only in very particular cases, we present the necessary conditions of optimality considering only a scalar constraint of the form $c(x(t)) \leq 0$, $\forall\, t \in [0\,, t_f]$. The optimal control problem (P_{tmin}) with a scalar state constraint can be written as the infinite dimensional minimization problem:

$$\min \{t_f \mid t_f > 0,\, u(\cdot) \in \mathcal{U},\, b \circ E_{x_0}(t_f, u(\cdot)) = 0,\, c \circ E_{x_0}(t, u(\cdot)) \leq 0,\, t \in [0\,, t_f]\}\,.$$

It is still possible to express necessary conditions in terms of Lagrange multipliers as before but this has to be done in distributions spaces and the Lagrange multipliers must be expressed as Radon measures (see e. g. [15]).

To emphasize the main difference with the state unconstrained case, we write the following optimization problem with only inequality constraints (we omit "$(\cdot)$" for readability):

$$\min_{u\in\mathcal{U}} J(u), \quad \text{subject to} \quad S(u)\leq 0.$$

Here S maps $\mathcal{U}$ into the Banach space of scalar-valued continuous function on $[0\,,t_f]$ denoted by $\mathrm{C}^0([0\,,t_f])$ and supplied with the uniform norm. According to [17, theorem 1], if J is a real-valued Fréchet differentiable function on $\mathcal{U}$ and $S\colon \mathcal{U}\to \mathrm{C}^0([0\,,t_f])$ a Fréchet differentiable mapping, then if $\bar u\in\mathcal{U}$ minimizes J subject to $S(\bar u)\leq 0$, then there exists a scalar $p^0\leq 0$, a linear form $\Lambda\in(\mathrm{C}^0([0\,,t_f]))^*$, $\Lambda\leq 0$ and non-increasing such that the Lagrangian $p^0J(u)+\langle\Lambda, S(u)\rangle$ is stationary at $\bar u$. Besides, $\langle\Lambda, S(\bar u)\rangle=0$ and from Riesz's theorem there exists a measure[4] $\bar\mu$ such that $\langle\Lambda, S(\bar u)\rangle=\int_0^{t_f} S(\bar u)\,\mathrm{d}\bar\mu$, where the integral is in the Stieltjes sense.

3.2. **Necessary optimality conditions**

We recall the necessary conditions due to [17] and [23] and follow the presentation of [8], which exhibits the role of the Lie bracket configuration.

3.2.1. *Definitions*

We call a *boundary arc*, labeled γ_c, an arc defined on an interval $I=[a\,,b]$ (not reduced to a singleton), such that $c(\gamma_c(t))=0$, for every $t\in I$. The times a and b are called the *entry-* and *exit-time* of the boundary arc; a and b are also termed *junction times*. An arc γ is said to have a *contact point* with the boundary at $\bar t\in[0\,,t_f]$ if $c(\gamma(\bar t))=0$ and $c(\gamma(t))<0$ for $t\neq\bar t$ in a neighborhood of $\bar t$. A subarc γ on which $c(\gamma(t))<0$ is called an *interior arc*.

The *generic order* of the constraint is the integer m such that $F_1\cdot c=F_1\cdot(F_0\cdot c)=\cdots=F_1\cdot(F_0^{m-2}\cdot c)=0$ and $F_1\cdot(F_0^{m-1}\cdot c)\neq 0$. If the order of a boundary arc γ_c is m, then its associated feedback control can be generically computed by differentiating m times the mapping $t\mapsto c(\gamma_c(t))$ and solving with respect to u the linear equation:

$$c^{(m)}=F_0^m\cdot c+u\,F_1\cdot(F_0^{m-1}\cdot c)=0.$$

A boundary arc is contained in $c=\dot c=\cdots=c^{(m)}=0$, and the constraint $c=0$ is called *primary* while the constraints $\dot c=\cdots=c^{(m)}=0$ are called *secondary*. The boundary feedback control is denoted by

$$u_c\coloneqq -\frac{F_0^m\cdot c}{F_1\cdot(F_0^{m-1}\cdot c)}.$$

3.2.2. *Assumptions*

Let $t\mapsto\gamma_c(t)$, $t\in[t_1\,,t_2]\subset[0\,,t_f]$, be a boundary arc associated with $u_c(\cdot)$. We introduce the assumptions:

- $(\mathbf{A_1})$ $(F_1\cdot(F_0^{m-1}\cdot c))(\gamma_c(t))\neq 0$ for $t\in[t_1\,,t_2]$, with m the order of the constraint.
- $(\mathbf{A_2})$ $|u_c(t)|\leq 1$ for $t\in[t_1\,,t_2]$, *i.e.* the boundary control is admissible.
- $(\mathbf{A_3})$ $|u_c(t)|<1$ for $t\in(t_1\,,t_2)$, *i.e.* the control is not saturating on the interior of the boundary arc.
- $(\mathbf{A_1^2})$ $(F_{01}\cdot c)(\gamma_c(t))\neq 0$ for $t\in[t_1\,,t_2]$.

Remark 3.1. Assumptions $\mathbf{A_1}$ and $\mathbf{A_1^2}$ are always satisfied for problem (P_{tmin}), see the proof of proposition 3.10. Assumption $\mathbf{A_2}$ is satisfied by any BC-extremals by definition. Assumption $\mathbf{A_3}$ is always satisfied for the constraint c_1 (see section 3.3.3 for the definition of c_1) of order 1 since $u_{c_1}(\cdot)$ is strictly increasing (see the

[4] In our case, $\bar\mu\leq 0$ because $p^0\leq 0$. In [17, theorem 1] $p^0\geq 0$ and $\bar\mu\geq 0$.

second item of section 5.3 page 24). About the constraint c_3 of order 2, for some limit cases, $u_{c_3}(\cdot) \equiv 1$. This can be seen on Figure 13 page 29.

3.2.3. *A maximum principle with a single state constraint*

Define the pseudo-Hamiltonian:

$$\begin{array}{rcl} H\colon T^*M \times U \times \mathbb{R} & \longrightarrow & \mathbb{R} \\ (x,p,u,\eta) & \longmapsto & H(x,p,u,\eta) \coloneqq \langle p, F_0(x) + u\,F_1(x)\rangle + \eta\, c(x), \end{array}$$

where η is the *Lagrange multiplier of the constraint.* Consider $(\bar{u}(\cdot), \bar{t}_f) \in \mathcal{U} \times \mathbb{R}_+^*$ an optimal solution with associated trajectory $\bar{x}(\cdot)$. Assume that the optimal control is piecewise smooth and that along each boundary arc, assumptions $\mathbf{A_1}$ and $\mathbf{A_2}$ are satisfied. Then we have the following necessary optimality conditions:

i) There exists a function $\bar{\eta}(\cdot) \leq 0$, a real number $p^0 \leq 0$ and a function $p(\cdot) \in BV([0\,,\bar{t}_f], (\mathbb{R}^n)^*)$ such that:

$$\dot{\bar{x}}(t) = \frac{\partial H}{\partial p}(\bar{x}(t), \bar{p}(t), \bar{u}(t), \bar{\eta}(t)), \quad \dot{\bar{p}}(t) = -\frac{\partial H}{\partial x}(\bar{x}(t), \bar{p}(t), \bar{u}(t), \bar{\eta}(t)), \quad t \in [0\,,\bar{t}_f] \text{ a.e.}$$

ii) The maximization condition holds for almost every $t \in [0\,,\bar{t}_f]$:

$$H(\bar{x}(t), \bar{p}(t), \bar{u}(t), \bar{\eta}(t)) = \max_{u \in U} H(\bar{x}(t), \bar{p}(t), u, \bar{\eta}(t)). \tag{5}$$

iii) The boundary conditions are satisfied and we have the following transversality conditions: $\bar{p}(\bar{t}_f) = (0, \mu, 0)$, $\mu \in \mathbb{R}$. Since t_f is free, if $\bar{u}(\cdot)$ is continuous at time $\bar{t}_f$, then $H(\bar{x}(\bar{t}_f), \bar{p}(\bar{t}_f), \bar{u}(\bar{t}_f), \bar{\eta}(\bar{t}_f)) = -p^0$.

iv) The function $\bar{\eta}(\cdot)$ is continuous on the interior of the boundary arcs and

$$\bar{\eta}(t)\, c(\bar{x}(t)) = 0, \quad \forall t \in [0\,,\bar{t}_f].$$

v) Let $\mathcal{T}$ denote the set of contact and junction times with the boundary. Then at $\tau \in \mathcal{T}$ we have

$$H[\tau^+] = H[\tau^-], \quad \text{where } [\tau] \text{ stands for } (\bar{x}(\tau), \bar{p}(\tau), \bar{u}(\tau), \bar{\eta}(\tau)), \tag{6}$$

$$\bar{p}(\tau^+) = \bar{p}(\tau^-) - \nu_\tau\, c'(\bar{x}(\tau)), \quad \text{where } \nu_\tau \coloneqq \bar{\mu}(\tau^+) - \bar{\mu}(\tau^-) \leq 0 \text{ (since } \bar{\mu} \text{ is non-increasing).} \tag{7}$$

Remark 3.2.

- In this context, an extremal is a quadruple $(x(\cdot), p(\cdot), u(\cdot), \eta(\cdot))$ satisfying i), ii), iv) and v). It is a BC-extremal if iii) also holds.
- On a boundary arc, the maximisation condition (5) with assumption $\mathbf{A_3}$ imply that $\Phi = 0$ on the interior of the boundary arc.
- The adjoint vector may be discontinuous at $\tau \in \mathcal{T}$, and $\bar{\eta}(\cdot) = \mathrm{d}\bar{\mu}(\cdot)/\,\mathrm{d}t$ on $[0\,,\bar{t}_f] \setminus \mathcal{T}$.

3.3. Computations of the multiplier and the jump and the junction conditions

We may find in [8, 23] the determination of the multiplier η and the jump ν_τ together with the analysis of the junction conditions, which is based on the concept of order and related to the classification of extremals. We give next some results for $m = 1$ and $m = 2$ since higher order constraints are not present in the problem (P_{tmin}).

3.3.1. *Case $m = 1$*

For a first-order constraint, assuming $\mathbf{A_1}$ and $\mathbf{A_3}$, we have the following lemma from [8].

Lemma 3.3. *Let $m = 1$. Then:*

i) along the boundary, $\eta = \dfrac{H_{01}}{F_1 \cdot c}$*;*
ii) if the control is discontinuous at a contact or junction time τ *of a bang arc with the boundary then* $\nu_\tau = 0$*.*
iii) we have

$$\nu_\tau = \frac{\Phi(\tau^-)}{(F_1 \cdot c)(x(\tau))} \text{ at an entry point and } \nu_\tau = -\frac{\Phi(\tau^+)}{(F_1 \cdot c)(x(\tau))} \text{ at an exit point.}$$

Proof. i) Along the boundary, $\Phi = 0$ since $\mathbf{A_3}$ is satisfied; differentiating, we obtain (with a slight abuse of notation)

$$0 = \dot{\Phi} = \{H, H_1\} = H_{01} + \eta\,\{c, H_1\} + c\,\{\eta, H_1\} = H_{01} - \eta\, F_1 \cdot c$$

and $F_1 \cdot c \neq 0$ along the boundary arc since $\mathbf{A_1}$ holds. Item i) is proved.
ii) See [8, lemma 2.4].
iii) According to (7), $p(\tau^+) = p(\tau^-) - \nu_\tau\, c'(x(\tau))$ at a junction point $x(\tau)$. If τ is an entry-time, then $\Phi(\tau^+) = H_1(x(\tau^+), p(\tau^+)) = \langle p(\tau^+), F_1(x(\tau^+))\rangle = 0$ and we have $0 = \Phi(\tau^-) - \nu_\tau(F_1 \cdot c)(x(\tau))$. The proof is similar at an exit-point.

□

Remark 3.4. The second item of lemma 3.3 is a particular case of [23, corollary 5.2] which states that if τ is a junction time between a bang arc and a boundary arc and if $m + r$ is odd, where r is the lowest order derivative of the optimal control which is discontinuous at τ, then $\nu_\tau = 0$. For this particular case where $m = 1$ and $r = 0$, it is still true even for a contact point (see lemma 3.3) but this is not proved in general in [23, corollary 5.2].

We profit from this lemma to get new junction conditions between bang and boundary arcs. We first need to define the sign of an arc. To do that, we first consider a non-empty arc γ_b defined on the interval $[t_0\,, t_1]$. We define the sign of the bang arc by $s_b \coloneqq \text{sign}(\Phi|_{\gamma_b})$, *i.e.* the sign of Φ on $(t_0\,, t_1)$, which is constant. In a same way, for a first-order constraint c, we define the sign of a non-empty arc γ_c by $s_c \coloneqq \text{sign}((F_1 \cdot c)|_{\gamma_c})$, assuming $\mathbf{A_1}$. Using these definitions, we have the following lemma which gives more insight into the junction conditions for the first-order case and which is necessary to define the multiple shooting function, see section 4.2.

Lemma 3.5. *Let consider two non-empty arcs* γ_b *and* γ_c*, with* c *a constraint of order 1, assume* $\mathbf{A_1}$ *and* $\mathbf{A_3}$ *along* γ_c *and note* $s_b = \text{sign}(\Phi|_{\gamma_b})$*,* $s_c = \text{sign}((F_1 \cdot c)|_{\gamma_c})$*. We note* τ *the junction time between* γ_b *and* γ_c *and* $z_\tau \in T^*M$ *its associated point.*

i) If the sequence is $\gamma_b\gamma_c$ *and*
  a) if $s_b\, s_c > 0$ *or* $z_{\tau^-} \in \Sigma_1^0$*, then* $\nu_\tau = 0$*, else*
  b) if $s_b\, s_c < 0$ *and* $z_{\tau^-} \notin \Sigma_1^0$*, then* $\nu_\tau < 0$ *(so the control is continuous at* τ*).*
ii) If the sequence is $\gamma_c\gamma_b$ *and*
  a) if $s_b\, s_c < 0$ *or* $z_{\tau^+} \in \Sigma_1^0$*, then* $\nu_\tau = 0$*, else*
  b) if $s_b\, s_c > 0$ *and* $z_{\tau^+} \notin \Sigma_1^0$*, then* $\nu_\tau < 0$ *(so the control is continuous at* τ*).*

Proof. Let prove first item *i-a)*. From lemma 3.3 and equation (7), at time τ we have

$$\frac{\Phi(\tau^-)}{(F_1 \cdot c)(x(\tau))} = \nu_\tau \leq 0,$$

and if $s_b\, s_c > 0$ then

$$\frac{\Phi(\tau^-)}{(F_1 \cdot c)(x(\tau))} \geq 0,$$

thus $\nu_\tau = 0$ and Φ is continuous at τ and $\Phi(\tau) = 0$. Item *i-a)* is proved. Now, if $s_b\, s_c < 0$ and $z_{\tau^-} \notin \Sigma_1^0$, then $\Phi(\tau^-) \neq 0$ and then $\nu_\tau < 0$. Item *i-b)* is proved. Items *ii-a)* and *ii-b)* are proved with the same argumentation. □

Remark 3.6. In the numerical results, see section 5, we have trajectories of the form $\gamma_+\gamma_{c_1}\gamma_+$, with $F_1 \cdot c_1 > 0$. By lemma 3.5, the jump is zero at the entry-time of γ_{c_1} and the control is continuous at the exit-time τ of γ_{c_1} if at $t = \tau^+$, the extremal has no contact with the switching surface.

3.3.2. *Case $m = 2$*

For a second-order constraint, assuming $\mathbf{A_1}$, $\mathbf{A_1^2}$ and $\mathbf{A_3}$, we have the following lemma.

Lemma 3.7. *Let $m = 2$. Then:*

i) along a boundary arc, we have $\eta = \dfrac{H_{001} + u_c\, H_{101}}{F_{01} \cdot c}$;

ii) at a contact or junction point at time τ, we have $\Phi(\tau^+) = \Phi(\tau^-)$;

iii) we have

$$\nu_\tau = \frac{\dot\Phi(\tau^-)}{(F_{01} \cdot c)(x(\tau))} \text{ at an entry point and } \nu_\tau = -\frac{\dot\Phi(\tau^+)}{(F_{01} \cdot c)(x(\tau))} \text{ at an exit point.}$$

For an order 2 constraint c, we define the sign of a non-empty arc γ_c by $s_c \coloneqq \operatorname{sign}((F_{01} \cdot c)|_{\gamma_c})$, assuming $\mathbf{A_1^2}$.

Lemma 3.8. *Let consider two non-empty arcs γ_b and γ_c, with c a constraint of order 2, assume $\mathbf{A_1}$, $\mathbf{A_1^2}$ and $\mathbf{A_3}$ along γ_c and note $s_b = \operatorname{sign}(\Phi|_{\gamma_b})$, $s_c = \operatorname{sign}((F_{01} \cdot c)|_{\gamma_c})$. We note τ the junction time between γ_b and γ_c and $z_\tau \in T^*M$ its associated point. For both sequences $\gamma_b\gamma_c$ and $\gamma_c\gamma_b$, if $s_b\, s_c < 0$ or $z_{\tau^-} \in \Sigma_{01}^0$, then $\nu_\tau = 0$, else if $s_b\, s_c > 0$ and $z_{\tau^-} \notin \Sigma_{01}^0$, then $\nu_\tau < 0$.*

Proof. Just notice that the signs of Φ and $\dot\Phi$ are equal after an exit point and are opposite before an entry point. Then, the proof is similar to the proof of lemma 3.5. □

Remark 3.9. In the numerical results, see section 5, we have trajectories with sequences of the form $\gamma_-\gamma_{c_3}$, with $F_{01} \cdot c_3 < 0$. By lemma 3.8, the jump is non zero at the junction if at this time, the extremal has no contact of order 2 with the switching surface.

3.3.3. *Application to problem (P_{tmin})*

Let define the space $C \coloneqq C_1 \cup C_3 \cup C_{13}$ where the boundary sets are $C_1 \coloneqq \{x \in M \mid |x_1| = 1,\ |x_3| \neq 1\}$, $C_3 \coloneqq \{x \in M \mid |x_1| \neq 1,\ |x_3| = 1\}$ and $C_{13} \coloneqq \{x \in M \mid |x_1| = |x_3| = 1\}$. For each state constraint, we write $c_i(x) \coloneqq s_i\, x_i - 1$, $i \in \{1, 3\}$, $s_i \in \{-1, 1\}$, and we label γ_{c_α}, $\alpha \in \{1, 3, 13\}$, a boundary arc defined on I such that for every $t \in I$, $\gamma_{c_\alpha}(t) \in C_\alpha$. Assuming $\mathbf{A_3}$, we have the following proposition.

Proposition 3.10. *We have:*

i) the constraint on the electric current, i.e. on x_1, is of order 1. The feedback boundary control and the multiplier associated to a boundary arc γ_{c_1} are given by:

$$u_{c_1}(x(t)) \coloneqq -\frac{1}{a_7}\left(a_1 s_1 + a_2 x_3(t)\right), \quad \eta_{c_1}(z(t)) \coloneqq -s_1 a_5\, p_3(t).$$

ii) the constraint on the angular velocity, i.e. on x_3, is of order 2. The feedback boundary control and the multiplier associated to a boundary arc γ_{c_3} are constant and given by:

$$u_{c_3}(x(t)) \coloneqq -\frac{1}{a_7}\left(-\frac{a_1\,(a_4 + a_6)}{a_5} + a_2 s_3\right), \quad \eta_{c_3}(z(t)) \coloneqq -s_3 a_3\, p_2.$$

Besides, on the boundary arc γ_{c_3} the electric current is constant and strictly positive and we have

$$x_1(\cdot) = -\frac{a_4 + a_6}{a_5} > 0.$$

iii) There exists boundary arcs $\gamma_{c_{13}}$ only if $a_4 + a_5 + a_6 = 0$ and if $\gamma_{c_{13}}$ is a boundary arc, then $s_1 = 1$ along $\gamma_{c_{13}}$.

Proof. i) Let consider a boundary arc γ_{c_1} defined on I. Then we have for every $t \in I$,

$$0 = \frac{\mathrm{d}}{\mathrm{d}t} c_1(\gamma_{c_1}(t)) = (F \cdot c_1)(\gamma_{c_1}(t)) = s_1 \left(a_1 x_1(t) + a_2 x_3(t)\right) + u(t)\, s_1\, a_7,$$

with $(F_1 \cdot c_1)\left(\gamma_{c_1}(t)\right) = s_1 a_7 \neq 0$ (so $\mathbf{A_1}$ is satisfied) and $x_1(t) = s_1$. Besides, $\eta_{c_1} = H_{01}/F_1 \cdot c_1$, *cf.* lemma 3.3 with H_{01} given at lemma 2.3 and $p_1 = 0$ along γ_{c_1} since $\mathbf{A_3}$ is assumed. Whence the results.

ii) Let consider a boundary arc γ_{c_3} defined on I. Then we have for every $t \in I$, $x_3(t) = s_3$ and

$$0 = \frac{\mathrm{d}}{\mathrm{d}t} c_3(\gamma_{c_3}(t)) = (F \cdot c_3)(\gamma_{c_3}(t)) = s_3 \left(a_4 + a_5 x_1(t) + a_6 x_3^2(t)\right) = s_3 \left(a_4 + a_5 x_1(t) + a_6\right).$$

The electric current is constant and strictly positive since $a_4 + a_5 x_1(t) + a_6 = 0$, with $a_4 < 0$, $a_5 > 0$ and $a_6 < 0$. Differentiating a second time we have

$$0 = \frac{\mathrm{d}^2}{\mathrm{d}t^2} c_3(\gamma_{c_3}(t)) = s_3 a_5\, \dot{x}_1(t) = s_3 a_5 \left(a_1 x_1(t) + a_2 x_3(t) + u(t) a_7\right), \quad x_3(t) = s_3,$$

with $(F_1 \cdot (F_0 \cdot c_3))\left(\gamma_{c_3}(t)\right) = s_3 a_5 a_7 \neq 0$, so $\mathbf{A_1}$ and $\mathbf{A_1^2}$ are satisfied since here $F_{01} \cdot c = -F_1 \cdot (F_0 \cdot c)$. The result follows with η_{c_3} given at lemma 3.7, H_{001}, H_{101} and F_{01} given at lemma 2.3, and with $p_1 = p_3 = 0$ along γ_{c_3} since $\mathbf{A_3}$ holds.

iii) According to *i*) and *ii*), on a boundary arc $\gamma_{c_{13}}$, $x_1 = s_1$ and $a_4 + a_5 x_1 + a_6 = 0$, $x_1 > 0$. Whence the result.

□

3.4. **Local time minimal synthesis**

We end this section with an application of theorem 4.4 from [8]. This theorem is local and valid only in the parabolic case. It asserts the following. One consider the time minimization problem for a 3-dimensional system of the form (2), $|u| \leq 1$, with the scalar constraint $c(x) \leq 0$. Let $\bar{x} \in c^{-1}(\{0\})$ and assume the following:

(1) at the point $\bar{x}$, the vectors F_0, F_1 and F_{01} form a frame and

$$[F_0 \pm F_1, F_{01}](\bar{x}) = a\, F_0(\bar{x}) + b\, F_1(\bar{x}) + c\, F_{01}(\bar{x}),$$

where $a > 0$;

(2) the constraint is of order 2 and assumptions $\mathbf{A_1}$ and $\mathbf{A_3}$ hold at the point $\bar{x}$.

Then the boundary arc passing through $\bar{x}$ is small time optimal if and only if the arc γ_+ is contained in the nonadmissible domain $c \geq 0$. In this case, the local time minimal synthesis with a boundary arc is of the form $\gamma_+ \gamma_-^T \gamma_c \gamma_-^T \gamma_+$, where γ_-^T are arcs tangent to the boundary arc. Therefore, we have the following proposition.

Proposition 3.11. *Let $\bar{x} \in c_3^{-1}(\{0\})$ with $s_3 = 1$, and assume $\mathbf{A_3}$ at the point $\bar{x}$. Assume also that the arc γ_+ passing through $\bar{x}$ is contained in the nonadmissible domain $c_3 \geq 0$. Then the local time minimal synthesis is of the form $\gamma_+ \gamma_-^T \gamma_{c_3} \gamma_-^T \gamma_+$.*

Proof. The constraint c_3 is of order 2, assumption $\mathbf{A_1}$ holds since $(F_1 \cdot (F_0 \cdot c_3))(\bar{x}) = a_5 a_7 \neq 0$ and $[F_0 \pm F_1, F_{01}](\bar{x}) = F_{001}(\bar{x}) = a\, F_0(\bar{x}) + b\, F_1(\bar{x}) + c\, F_{01}(\bar{x})$, with $a = a_5 a_7 / \bar{x}_3 > 0$. □

4. Numerical methods

In this section, we present the numerical methods used to find BC-extremals of problem (P_{tmin}). All the methods are implemented within the `HamPath` code, see [11]. The software is based upon indirect methods: simple, multiple shooting, differential path following (or homotopy) methods and exponential mappings. One focus on the description of the shooting and homotopic functions, the methods being automatically generated by the `HamPath` code. One pay a special attention in section 4.2 on the strategy we develop to define the shooting functions associated to problems with state constraints.

Remark 4.1. From now on, the state constraints are $c_1(x) = x_1 - 1$ and $c_3(x) = x_3 - 1$.

Remark 4.2. We only present the shooting functions associated to the structures we encounter in section 5.3 during numerical experiments.

4.1. Simple shooting method

4.1.1. *Structure* γ_+

If $i_{\max}$ and $\omega_{\max}$ (or $v_{\max} = \omega_{\max} \times 3.6\, r/K_r$) are big enough the solution of problem (P_{tmin}) has only interior arcs and then the optimal trajectory is of the form γ_+, see proposition 2.11. We need the following definitions.

Definition 4.3. For fixed $\bar{z}_0 \in T^*M$ and $\bar{t} \geq 0$, we define in a neighborhood of $(\bar{z}_0, \bar{t})$ (if possible), the following *exponential mapping* $(z_0, t) \mapsto \exp(t\overrightarrow{H})(z_0)$ as the trajectory $z(\cdot)$ at time t of the Hamiltonian vector $\overrightarrow{H}$, *i.e.* $\dot{z}(s) = \overrightarrow{H}(z(s))$ for every $s \in [0\,, t]$, satisfying $z(0) = z_0$.

Definition 4.4. Let $\overrightarrow{H}$ be a Hamiltonian vector on T^*M, and let $z(\cdot)$ be a trajectory of $\overrightarrow{H}$ defined on $[0\,, t_f]$. The differential equation on $[0\,, t_f]$

$$\dot{\overrightarrow{\delta z}}(t) = \mathrm{d}\overrightarrow{H}(z(t)) \cdot \delta z(t)$$

is called a *Jacobi equation*, or *variational system*, along $z(\cdot)$. Let $\delta z(\cdot)$ be a solution of the variational system along $z(\cdot)$, we write $\delta z(t) =: \exp(t\, \mathrm{d}\overrightarrow{H}|_{z(\cdot)})(\delta z(0))$.

Let $(z(\cdot), u(\cdot))$ be a regular extremal defined on $[0\,, t_f]$ with only one single positive bang arc. We have $z(t) = \exp(t\overrightarrow{H_+})(z(0))$, $t \in [0\,, t_f]$, where $H_+(z) = H(z, u(z)) = H_0(z) + H_1(z)$. Let denote by π the following projection: in coordinates, writing $z \coloneqq (x, p) \in T^*M$, then $\pi(z) \coloneqq (x_2, p_1, p_3)$. We define now the *simple shooting function*

$$S_1(p_0, t_f) \coloneqq \begin{pmatrix} \pi\left(\exp(t_f \overrightarrow{H_+})(z_0)\right) \\ H_+\left(\exp(t_f \overrightarrow{H_+})(z_0)\right) \end{pmatrix} - \begin{pmatrix} 1 \\ 0 \\ 0 \\ 1 \end{pmatrix},$$

where $z_0 \coloneqq (x_0, p_0)$, with $x_0 = (0, 0, 0)$ fixed. If $(\bar{p}_0, \bar{t}_f)$ is a zero of S_1, then the constant control $u(\cdot) = +1$ with the integral curve $t \mapsto \exp(t\overrightarrow{H_+})(\bar{z}_0)$, with $\bar{z}_0 \coloneqq (x_0, \bar{p}_0)$, for $t \in [0\,, \bar{t}_f]$, is a BC-extremal, *i.e.* the extremal satisfies the necessary optimality conditions, see section 2.1. The *simple shooting method* consists in finding a zero of the simple shooting function S_1, *i.e.* in solving $S_1(p_0, t_f) = 0$.

4.1.2. *`HamPath` code*

The Fortran hybrid Newton method `hybrj` (from the `minpack` library [25]) is used to solve the nonlinear system $S_1(p_0, t_f) = 0$. Providing H_+ and S_1 to `HamPath`, the code generates automatically the Jacobian of the shooting function given to the solver. To make the implementation of S_1 easier, `HamPath` supplies the exponential mapping. Automatic Differentiation (`tapenade` software [16]) is used to produce $\overrightarrow{H_+}$ and is combined with Runge-Kutta integrators (`dopri5`, `dop853`, see [13] and `radau`, see [14]) to assemble the exponential mapping.

We detail how the Jacobian of the shooting function is computed. If we note $z(t, z_0) \coloneqq \exp(t\overrightarrow{H_+})(z_0)$, then the Jacobian is given by

$$\frac{\partial S_1}{\partial p_0}(p_0, t_f)\,\delta p_0 = \begin{pmatrix} \mathrm{d}\pi\,(z(t_f, z_0)) \cdot \dfrac{\partial z}{\partial z_0}(t_f, z_0)\,\delta z_0 \\ \mathrm{d}H_+\,(z(t_f, z_0)) \cdot \dfrac{\partial z}{\partial z_0}(t_f, z_0)\,\delta z_0 \end{pmatrix}, \quad \delta z_0 \coloneqq \begin{pmatrix} 0_{\mathbb{R}^n} \\ \delta p_0 \end{pmatrix}, \quad \delta p_0 \in \mathbb{R}^n,$$

$$\frac{\partial S_1}{\partial t_f}(p_0, t_f)\,\delta t_f = \delta t_f \begin{pmatrix} \mathrm{d}\pi\,(z(t_f, z_0)) \cdot \overrightarrow{H_+}(z(t_f, z_0)) \\ \mathrm{d}H_+\,(z(t_f, z_0)) \cdot \overrightarrow{H_+}(z(t_f, z_0)) \end{pmatrix}, \quad \delta t_f \in \mathbb{R},$$

where

$$\frac{\partial z}{\partial z_0}(t_f, z_0)\,\delta z_0 = \exp(t_f\,\mathrm{d}\overrightarrow{H_+}|_{z(\cdot, z_0)})(\delta z_0),$$

and $\mathrm{d}H_+\,(z(t_f, z_0)) \cdot \overrightarrow{H_+}(z(t_f, z_0)) = \{H_+, H_+\}(z(t_f, z_0)) = 0$. To assemble automatically the Jacobian, `HamPath` uses AD to compute $\mathrm{d}\pi$, $\mathrm{d}H_+$ and $\mathrm{d}\overrightarrow{H_+}$, and produces the exponential mapping associated to the variational system.

4.2. **Multiple shooting method**

We need the following propositions (inspired by [1, lemma 20.21] and [12, proposition 1]) to define the shooting functions when the solutions have boundary arcs. We introduce for that the canonical x-projection: $\pi_x(x, p) \coloneqq x$, $(x, p) \in T^*M$.

Proposition 4.5. *Let $c(x) \leq 0$ be a scalar constraint of order 1, and define for $z \coloneqq (x, p) \in T^*M$ the true Hamiltonian*

$$H_c(z) \coloneqq H(z, u_c(x), \eta_c(z)) = H_0(z) + u_c(x)\,H_1(z) + \eta_c(z)\,c(x),$$

with

$$u_c(x) = -\frac{(F_0 \cdot c)(x)}{(F_1 \cdot c)(x)}, \quad \eta_c(z) = \frac{H_{01}(z)}{(F_1 \cdot c)(x)}.$$

Let $\bar{z} \coloneqq (\bar{x}, \bar{p}) \in \Sigma_1^0$, $c(\bar{x}) = 0$; there is exactly one extremal $(x(\cdot), p(\cdot), u(\cdot), \eta(\cdot))$ passing through $\bar{z}$, such that $c \circ x(\cdot) = 0$, $H_1 \circ z(\cdot) = 0$, $z(\cdot) \coloneqq (x(\cdot), p(\cdot))$, and it is defined by the flow of H_c.

Proof. First we show that the space $\{x \in M \mid c(x) = 0\} \cap \Sigma_1^0$ is invariant with respect to the flow of H_c. Let $\bar{z} \coloneqq (\bar{x}, \bar{p}) \in \Sigma_1^0$, $c(\bar{x}) = 0$, and let $z(\cdot) \coloneqq (x(\cdot), p(\cdot))$ be the associated integral curve of H_c passing through $\bar{z}$ at time 0. Let $\varphi \coloneqq (g, H_1) \circ z(\cdot)$, with $g \coloneqq c \circ \pi_x$; then φ is differentiable and

$$\begin{aligned}
\dot{\varphi}_1(t) &= \{H_c, g\}(z(t)) \\
&= \Big(\underbrace{\{H_0, g\} + \{H_1, g\}\,(u_c \circ \pi_x)}_{=0 \text{ by definition of } u_c} + \underbrace{\{u_c \circ \pi_x, g\}}_{=0}\,H_1 + \underbrace{\{c \circ \pi_x, g\}}_{=0}\,\eta_c + \{\eta_c, g\}\,(c \circ \pi_x) \Big)(z(t)). \\
\dot{\varphi}_2(t) &= \{H_c, H_1\}(z(t)) \\
&= \Big(\underbrace{H_{01} + \{c \circ \pi_x, H_1\}\,\eta_c}_{=0 \text{ by definition of } \eta_c} + \underbrace{\{H_1, H_1\}}_{=0}\,(u_c \circ \pi_x) + \{u_c \circ \pi_x, H_1\}\,H_1 + \{\eta_c, H_1\}\,(c \circ \pi_x) \Big)(z(t)).
\end{aligned}$$

so $\dot{\varphi}(t) = A(t)\,\varphi(t)$, with

$$A(t) \coloneqq \begin{bmatrix} \{\eta_c, c \circ \pi_x\} & 0 \\ \{\eta_c, H_1\} & \{u_c \circ \pi_x, H_1\} \end{bmatrix}(z(t)).$$

Since $\varphi(0) = 0$, φ is indentically zero and $z(\cdot)$ remains in $\{x \in M \mid c(x) = 0\} \cap \Sigma_1^0$. Now,

$$H_c'(z) = \frac{\partial H}{\partial z}(z, u_c(x), \eta_c(z)) + \frac{\partial H}{\partial u}(z, u_c(x), \eta_c(z))\,(u_c \circ \pi_x)'(z) + \frac{\partial H}{\partial \eta}(z, u_c(x), \eta_c(z))\,\eta_c'(z),$$

with

$$\frac{\partial H}{\partial u}(z, u_c(x), \eta_c(z)) = H_1(z) \quad \text{and} \quad \frac{\partial H}{\partial \eta}(z, u_c(x), \eta_c(z)) = c(x),$$

so $\overrightarrow{H_c}(z(t)) = \overrightarrow{H}(z(t), u_c(x(t)), \eta_c(z(t)))$ as H_1 and $c \circ \pi_x$ vanish along $z(\cdot)$, and $(z(\cdot), u_c \circ x(\cdot), \eta_c \circ z(\cdot))$ is extremal. □

For the second-order case, we have the following proposition.

Proposition 4.6. *Let $c(x) \leq 0$ be a scalar constraint of order 2, and define for $z \coloneqq (x, p) \in T^*M$ the true Hamiltonian*

$$H_c(z) \coloneqq H(z, u_c(x), \eta_c(z)) = H_0(z) + u_c(x)\,H_1(z) + \eta_c(z)\,c(x),$$

with

$$u_c(x) = -\frac{(F_0^2 \cdot c)(x)}{(F_1 \cdot (F_0 \cdot c))(x)}, \quad \eta_c(z) = \frac{H_{001}(z) + u_c(x)\,H_{101}(z)}{(F_{01} \cdot c)(x)}.$$

i) Assume that the control is constant, i.e. $\forall x \in M$, $u_c'(x) = 0$. Let $\bar{z} \coloneqq (\bar{x}, \bar{p}) \in T^*M$, $c(\bar{x}) = 0$ and $(F_0 \cdot c)(\bar{x}) = 0$; there is exactly one extremal $(x(\cdot), p(\cdot), u(\cdot), \eta(\cdot))$ passing through $\bar{z}$, such that

$$c \circ x(\cdot) = 0 \quad \textit{and} \quad (F_0 \cdot c) \circ x(\cdot) = 0,$$

and it is defined by the flow of H_c.

ii) Let $\bar{z} \coloneqq (\bar{x}, \bar{p}) \in \Sigma_1^0 \cap \Sigma_{01}^0$, $c(\bar{x}) = 0$ and $(F_0 \cdot c)(\bar{x}) = 0$; there is exactly one extremal $(x(\cdot), p(\cdot), u(\cdot), \eta(\cdot))$ passing through $\bar{z}$, such that

$$c \circ x(\cdot) = 0, \quad (F_0 \cdot c) \circ x(\cdot) = 0, \quad H_1 \circ z(\cdot) = 0 \quad \textit{and} \quad H_{01} \circ z(\cdot) = 0,$$

$z(\cdot) \coloneqq (x(\cdot), p(\cdot))$, and it is defined by the flow of H_c.

Proof. First we show that the spaces

$$E_1 \coloneqq \{x \in M \mid c(x) = 0\} \cap \{x \in M \mid (F_0 \cdot c)(x) = 0\} \quad \text{and} \quad E_2 \coloneqq E_1 \cap \Sigma_1^0 \cap \Sigma_{01}^0 = E_1 \cap \Sigma_s$$

are invariant with respect to the flow of H_c. Let $\bar{z} \coloneqq (\bar{x}, \bar{p}) \in T^*M$, and let $z(\cdot) \coloneqq (x(\cdot), p(\cdot))$ be the associated integral curve of H_c passing through $\bar{z}$ at time 0. Let $\varphi \coloneqq (g, f, H_1, H_{01}) \circ z(\cdot)$, with $g \coloneqq c \circ \pi_x$ and $f \coloneqq (F_0 \cdot c) \circ \pi_x$;

then φ is differentiable and we have the following.

$$\begin{aligned}
\dot\varphi_1(t) &= \{H_c, g\}(z(t)) \\
&= \Big(\{H_0, g\} + \underbrace{\{H_1, g\}\,(u_c\circ\pi_x)}_{=0 \text{ (c of order 2)}} + \underbrace{\{u_c\circ\pi_x, g\}}_{=0}\, H_1 + \underbrace{\{c\circ\pi_x, g\}}_{=0}\,\eta_c + \{\eta_c, g\}\,(c\circ\pi_x)\Big)(z(t)) \\
&= \Big((F_0\cdot c)\circ\pi_x + \{\eta_c, g\}\,(c\circ\pi_x)\Big)(z(t)), \\
\dot\varphi_2(t) &= \{H_c, f\}(z(t)) \\
&= \Big(\underbrace{\{H_0, f\} + \{H_1, f\}\,(u_c\circ\pi_x)}_{=0 \text{ by definition of } u_c} + \underbrace{\{u_c\circ\pi_x, f\}}_{=0}\, H_1 + \underbrace{\{c\circ\pi_x, f\}}_{=0}\,\eta_c + \{\eta_c, f\}\,(c\circ\pi_x)\Big)(z(t)), \\
\dot\varphi_3(t) &= \{H_c, H_1\}(z(t)) \\
&= \Big(H_{01} + \underbrace{\{H_1, H_1\}}_{=0}\,(u_c\circ\pi_x) + \{u_c\circ\pi_x, H_1\}\, H_1 + \underbrace{\{c\circ\pi_x, H_1\}}_{=0}\,\eta_c + \{\eta_c, H_1\}\,(c\circ\pi_x)\Big)(z(t)), \\
\dot\varphi_4(t) &= \{H_c, H_{01}\}(z(t)) \\
&= \Big(\underbrace{H_{001} + H_{101}\,(u_c\circ\pi_x) + \{c\circ\pi_x, H_{01}\}\,\eta_c}_{=0 \text{ by definition of } \eta_c} + \{u_c\circ\pi_x, H_{01}\}\, H_1 + \{\eta_c, H_{01}\}\,(c\circ\pi_x)\Big)(z(t)),
\end{aligned}$$

so $\dot\varphi(t) = A(t)\,\varphi(t)$, with

$$A(t) \coloneqq \begin{bmatrix} \{\eta_c, g\} & 1 & 0 & 0 \\ \{\eta_c, f\} & 0 & 0 & 0 \\ \{\eta_c, H_1\} & 0 & \{u_c\circ\pi_x, H_1\} & 1 \\ \{\eta_c, H_{01}\} & 0 & \{u_c\circ\pi_x, H_{01}\} & 0 \end{bmatrix}(z(t)),$$

and we have also

$$\begin{bmatrix} \dot\varphi_1(t) \\ \dot\varphi_2(t) \end{bmatrix} = \begin{bmatrix} \{\eta_c, g\}(z(t)) & 1 \\ \{\eta_c, f\}(z(t)) & 0 \end{bmatrix} \begin{bmatrix} \varphi_1(t) \\ \varphi_2(t) \end{bmatrix}.$$

So if $\varphi_1(0) = \varphi_2(0) = 0$, *i.e.* $\bar z \in E_1$, then φ_1 and φ_2 are indentically zero and $z(\cdot)$ remains in E_1. Now if $\varphi(0) = 0$, *i.e.* $\bar z \in E_2$, then φ is indentically zero and $z(\cdot)$ remains in E_2. Now,

$$H_c'(z) = \frac{\partial H}{\partial z}(z, u_c(x), \eta_c(z)) + \frac{\partial H}{\partial u}(z, u_c(x), \eta_c(z))\,(u_c\circ\pi_x)'(z) + \frac{\partial H}{\partial \eta}(z, u_c(x), \eta_c(z))\,\eta_c'(z),$$

with

$$\frac{\partial H}{\partial u}(z, u_c(x), \eta_c(z)) = H_1(z) \quad \text{and} \quad \frac{\partial H}{\partial \eta}(z, u_c(x), \eta_c(z)) = c(x),$$

so

- if $\bar z \in E_1$ and if we assume $(u_c\circ\pi_x)' = 0$ then $\overrightarrow{H_c}(z(t)) = \overrightarrow{H}(z(t), u_c(x(t)), \eta_c(z(t)))$ as $z(\cdot)$ remains in E_1, and $(z(\cdot), u_c\circ x(\cdot), \eta_c\circ z(\cdot))$ is extremal. Item i) is proved.
- if $\bar z \in E_2$ then $\overrightarrow{H_c}(z(t)) = \overrightarrow{H}(z(t), u_c(x(t)), \eta_c(z(t)))$ as $z(\cdot)$ remains in E_2, and $(z(\cdot), u_c\circ x(\cdot), \eta_c\circ z(\cdot))$ is extremal. Item ii) is proved.

□

4.2.1. *Structure $\gamma_+\gamma_{c_1}\gamma_+$ and limit case $\gamma_+^{c_1}$*

We introduce for $z \coloneqq (x,p) \in T^*M$ the true Hamiltonian

$$H_{c_1}(z) \coloneqq H(z, u_{c_1}(x), \eta_{c_1}(z)) = H_0(z) + u_{c_1}(x)\, H_1(z) + \eta_{c_1}(z)\, c_1(x),$$

where $c_1(x) = x_1 - 1$, and u_{c_1} and η_{c_1} are given by proposition 3.10. Here we consider a trajectory with a structure of the form $\gamma_+\gamma_{c_1}\gamma_+$, with non-empty arcs. We note $t_1 < t_2$ the junction times. To define the *multiple shooting function* associated to this structure, we need the results about the transversality conditions and the level of the Hamiltonian from section 2.1, and we use also lemmas 3.3, 3.5 and proposition 4.5. We assume that $\mathbf{A_3}$ holds along γ_{c_1}, and that at t_2, there is no contact with the switching surface. Then, since $F_1 \cdot c_1 \equiv a_7 > 0$, then $\mathbf{A_1}$ is also satisfied, and from lemma 3.5 we have at t_1, $\nu_1 = 0$, and at t_2, $\nu_2 < 0$ and the control is continuous at t_2. Proposition 4.5 gives two conditions at time t_1: $c_1(\pi_x(z_1)) = H_1(z_1) = 0$. The multiple shooting function $S_2(p_0, t_f, t_1, t_2, \nu_2, z_1, z_2)$ is then given by the following equations.

$$\begin{aligned}
&0 = c_1(\pi_x(z_1)), && 0 = H_1(z_1), && 1 = u_{c_1}(\pi_x(z_2)),\\
&(1,0,0) = \pi\left(\exp((t_f - t_2)\overrightarrow{H_+})(z_2^+)\right), && 1 = H_+\left(\exp((t_f - t_2)\overrightarrow{H_+})(z_2^+)\right),\\
&0 = \exp(t_1\overrightarrow{H_+})(z_0) - z_1, && 0 = \exp((t_2 - t_1)\overrightarrow{H_{c_1}})(z_1) - z_2,
\end{aligned}$$

where $z_0 \coloneqq (x_0, p_0)$, $x_0 = (0,0,0)$ is fixed, $z_2^+ \coloneqq z_2 - \nu_2\, c_1'(\pi_x(z_2))\frac{\partial}{\partial p}$. The last two equations are classical matching conditions: see [10] for details about multiple shooting methods. The *multiple shooting method* in the case of structure $\gamma_+\gamma_{c_1}\gamma_+$ consists in finding a zero of the multiple shooting function S_2, *i.e.* in solving

$$S_2(p_0, t_f, t_1, t_2, \nu_2, z_1, z_2) = 0.$$

A zero of the shooting function $S_2 = 0$ gives a BC-extremal of the form $\gamma_+\gamma_{c_1}\gamma_+$ which satisfies the necessary conditions of optimality of section 3.2.3.

Limit case $\gamma_+^{c_1}$. In the limit case where $t_1 = t_2$, we have a contact with the boundary C_1 instead of a junction. We note $\gamma_+^{c_1}$ an arc γ_+ with a contact point with C_1.

4.2.2. *Structure $\gamma_+\gamma_{c_1}\gamma_+\gamma_-\gamma_+^{c_3}$ and limit case $\gamma_+\gamma_{c_1}\gamma_+^{H_1,c_3}$*

We define the multiple shooting function S_3 associated to the structure $\gamma_+\gamma_{c_1}\gamma_+\gamma_-\gamma_+^{c_3}$. We assume that $\mathbf{A_3}$ holds along γ_{c_1}, and that at t_2 (the exit-time of γ_{c_1}), there is no contact with the switching surface. The last bang arc has a contact point with the boundary C_3 so is labeled $\gamma_+^{c_3}$. The multiple shooting function $S_3(p_0, t_f, t_1, t_2, \nu_2, t_3, t_4, t_5, \nu_5, z_1, z_2, z_3, z_4, z_5)$ is defined by the following equations.

$$\begin{aligned}
&0 = c_1(\pi_x(z_1)), && 0 = H_1(z_1), && 1 = u_{c_1}(\pi_x(z_2)),\\
&0 = H_1(z_3), && 0 = H_1(z_4), &&\\
&0 = c_3(\pi_x(z_5)), && 0 = (F_0 \cdot c_3)(\pi_x(z_5)), &&\\
&(1,0,0) = \pi\left(\exp((t_f - t_5)\overrightarrow{H_+})(z_5^+)\right), && 1 = H_+\left(\exp((t_f - t_5)\overrightarrow{H_+})(z_5^+)\right), &&\\
&0 = \exp(t_1\overrightarrow{H_+})(z_0) - z_1, && 0 = \exp((t_2 - t_1)\overrightarrow{H_{c_1}})(z_1) - z_2, && 0 = \exp((t_3 - t_2)\overrightarrow{H_+})(z_2^+) - z_3,\\
&0 = \exp((t_4 - t_3)\overrightarrow{H_-})(z_3) - z_4, && 0 = \exp((t_5 - t_4)\overrightarrow{H_+})(z_4) - z_5, &&
\end{aligned}$$

where $z_0 \coloneqq (x_0, p_0)$, $x_0 = (0,0,0)$ is fixed, $z_2^+ \coloneqq z_2 - \nu_2\, c_1'(\pi_x(z_2))\frac{\partial}{\partial p}$, and $z_5^+ \coloneqq z_5 - \nu_5\, c_3'(\pi_x(z_5))\frac{\partial}{\partial p}$. The *multiple shooting method* in the case of structure $\gamma_+\gamma_{c_1}\gamma_+\gamma_-\gamma_+^{c_3}$ consists in finding a zero of the multiple shooting function S_3, *i.e.* in solving

$$S_3(p_0, t_f, t_1, t_2, \nu_2, t_3, t_4, t_5, \nu_5, z_1, z_2, z_3, z_4, z_5) = 0,$$

and we get a BC-extremal of the form $\gamma_+\gamma_{c_1}\gamma_+\gamma_-\gamma_+^{c_3}$.

Limit case $\gamma_+\gamma_{c_1}\gamma_+^{H_1,c_3}$. In the limit case where $t_3 = t_4$, we have a contact of order 2 with the switching surface instead of two consecutive contacts of order 1, see 2.4.2. We note $\gamma_+^{H_1,c_3}$ an arc γ_+ with a contact point of order 2 with the switching surface defined by $H_1 = 0$ followed by a contact point with C_3. In this case, we have one unknown τ instead of two (t_3 and t_4), with associated point z_τ (instead of z_3 and z_4) but we may add as extra unknown the parameter $v_{\max}$; all others parameters from w remain fixed. Now, we may replace $H_1(z_3) = H_1(z_4) = 0$ by $H_1(z_\tau) = H_{01}(z_\tau) = 0$.

4.2.3. *Structure* $\gamma_+\gamma_{c_1}\gamma_+\gamma_-\gamma_{c_3}$

We introduce for $z \coloneqq (x,p) \in T^*M$ the true Hamiltonian

$$H_{c_3}(z) \coloneqq H(z, u_{c_3}(x), \eta_{c_3}(z)) = H_0(z) + u_{c_3}(x)\, H_1(z) + \eta_{c_3}(z)\, c_3(x),$$

where $c_3(x) = x_3 - 1$, and u_{c_3} and η_{c_3} are given by proposition 3.10. We define now the multiple shooting function S_4 associated to the strucutre $\gamma_+\gamma_{c_1}\gamma_+\gamma_-\gamma_{c_3}$, We assume that $\mathbf{A_3}$ holds along γ_{c_1} and γ_{c_3} ($\mathbf{A_1}$ is satisfied along γ_{c_1} and γ_{c_3}), and that at t_2 (the exit-time of γ_{c_1}), there is no contact with the switching surface. We use propositions 4.5 and 4.6 and lemmas 3.3, 3.5, 3.7 and 3.8 with the results from section 2.1 to get the multiple shooting function S_4. One can recall that the transversality conditions $p_1(t_f) = p_3(t_f) = 0$ are equivalent to $\Phi(t_f) = \dot\Phi(t_f) = 0$, and that the control is constant along γ_{c_3}. Then according to proposition 4.6, we only need to check that c_3 and $F_0 \cdot c_3$ are zero at the entry-time of γ_{c_3}. The following equations describe the multiple shooting function $S_4(p_0, t_f, t_1, t_2, \nu_2, t_3, t_4, \nu_4, z_1, z_2, z_3, z_4)$.

$$
\begin{aligned}
&0 = c_1\left(\pi_x\left(z_1\right)\right), && 0 = H_1\left(z_1\right), && 1 = u_{c_1}\left(\pi_x\left(z_2\right)\right),\\
&0 = H_1\left(z_3\right), &&&&\\
&0 = c_3\left(\pi_x\left(z_4\right)\right), && 0 = (F_0 \cdot c_3)(\pi_x\left(z_4\right)), &&\\
&(1,0,0) = \pi\left(\exp((t_f - t_4)\overrightarrow{H_+})(z_4^+)\right), && 1 = H_+\left(\exp((t_f - t_4)\overrightarrow{H_+})(z_4^+)\right), &&\\
&0 = \exp(t_1\overrightarrow{H_+})(z_0) - z_1, && 0 = \exp((t_2 - t_1)\overrightarrow{H_{c_1}})(z_1) - z_2, && 0 = \exp((t_3 - t_2)\overrightarrow{H_+})(z_2^+) - z_3,\\
&0 = \exp((t_4 - t_3)\overrightarrow{H_-})(z_3) - z_4, &&&&
\end{aligned}
$$

where $z_0 \coloneqq (x_0, p_0)$, $x_0 = (0,0,0)$ fixed, $z_2^+ \coloneqq z_2 - \nu_2\, c_1'(\pi_x(z_2))\frac{\partial}{\partial p}$, and $z_4^+ \coloneqq z_4 - \nu_4\, c_3'(\pi_x(z_4))\frac{\partial}{\partial p}$. The *multiple shooting method* in the case of structure $\gamma_+\gamma_{c_1}\gamma_+\gamma_-\gamma_{c_3}$ consists in finding a zero of the multiple shooting function S_4, *i.e.* in solving

$$S_4(p_0, t_f, t_1, t_2, \nu_2, t_3, t_4, \nu_4, z_1, z_2, z_3, z_4) = 0,$$

and we get a BC-extremal of the form $\gamma_+\gamma_{c_1}\gamma_+\gamma_-\gamma_{c_3}$.

Limit case $\gamma_+\gamma_{c_1}\gamma_+\gamma_-\gamma_{c_3}$ with $u_{c_3}(\cdot) \equiv +1$. This is a particular case when the boundary and regular arcs are identical. This phenomenon happens at the interface between $\gamma_+\gamma_{c_1}\gamma_+\gamma_-\gamma_+^{c_3}$ and $\gamma_+\gamma_{c_1}\gamma_+\gamma_-\gamma_{c_3}$ (with $u_{c_3} < 1$) trajectories, see section 3.4.

Limit case $\gamma_+\gamma_{c_1}\gamma_+\gamma_-\gamma_{c_3}$ with $t_2 = t_3$. In the limit case when $t_2 = t_3$, we have a trajectory of the form $\gamma_+\gamma_{c_1}\gamma_-\gamma_{c_3}$. From S_4, it is straightforward to obtain the multiple shooting function S_5 associated to the structure $\gamma_+\gamma_{c_1}\gamma_-\gamma_{c_3}$.

4.2.4. *`HamPath` code*

For any case presented in section 4.2, the user must provide the true Hamiltonians and the shooting function. The `HamPath` code supply automatically (by AD and integrating the Hamiltonian and variational systems) the exponential mappings, the Jacobian of the shooting function and the nonlinear solver.

4.3. **Differential path following method**

The shooting method solves a single optimal control problem, *i.e.* all the parameters in w are fixed. To solve a one-parameter family of optimal control problems, *e.g.* for different values of $w_{10} = i_{\max}$, we use differential path following techniques with arclength parametrization (or homotopy method). Let $h\colon \mathbb{R}^N \times \mathbb{R} \to \mathbb{R}^N$, $h(y, \lambda)$, denote an homotopic function. For example, one can consider the homotopic function defined by S_1, with $y \coloneqq (p_0, t_f)$, $N = 4$ and $\lambda \coloneqq w_{10}$ ($i_{\max}$ is here an independent variable). We are interested in solving $h = 0$. Under some assumptions, the solutions set forms a one-dimensional manifold.

The classical difficulties about homotopic methods consist in assuring that a curve in $h^{-1}(\{0\})$ exists, is sufficiently smooth and will intersect a fixed target homotopic level in finite length. Suppose h is continuously differentiable and that we know y_0 such that $h(y_0, \lambda_0) = 0$ and

$$\operatorname{rank}\left(\frac{\partial h}{\partial y}(y_0, \lambda_0)\right) = N.$$

Suppose also that 0 is a regular value of h. Then a continuously differentiable curve starting from (y_0, λ_0) exists and is either diffeomorphic to a circle or the real line. The curves in $h^{-1}(\{0\})$ are disjoints, and we call each branch of $h^{-1}(\{0\})$ a path of zeros.

Unlike well-known prediction-correction methods, see [2], the `HamPath` code implements an algorithm which merely follow the path of zeros by integrating the associated differential system with a high order Runge-Kutta scheme, without any correction. The key point is to compute efficiently the Jacobian of the homotopic function with the tools presented in section 4.1.2. See [7, 11] for more details about the algorithm.

We group together in Table 2, the different homotopies we need for the numerical results.

Shooting fun.	Homotopic fun.	Structure	Homotopic par.
$S_1(p_0, t_f)$	h_1	γ_+	$i_{\max}$
$S_2(p_0, t_f, t_1, t_2, \nu_2, z_1, z_2)$	$h_2^{(a)}$	$\gamma_+\gamma_{c_1}\gamma_+$	$i_{\max}$
$S_2(p_0, t_f, t_1, t_2, \nu_2, z_1, z_2)$	$h_2^{(b)}$	$\gamma_+\gamma_{c_1}\gamma_+$	$v_{\max}$
$S_3(p_0, t_f, t_1, t_2, \nu_2, t_3, t_4, t_5, \nu_5, z_1, z_2, z_3, z_4, z_5)$	h_3	$\gamma_+\gamma_{c_1}\gamma_+\gamma_-\gamma_+^{c_3}$	$v_{\max}$
$S_4(p_0, t_f, t_1, t_2, \nu_2, t_3, t_4, \nu_4, z_1, z_2, z_3, z_4)$	h_4	$\gamma_+\gamma_{c_1}\gamma_+\gamma_-\gamma_{c_3}$	$v_{\max}$
$S_5(p_0, t_f, t_1, t_2, t_3, \nu_3, z_1, z_2, z_3)$	h_5	$\gamma_+\gamma_{c_1}\gamma_-\gamma_{c_3}$	$v_{\max}$

TABLE 2. The homotopic function name with the associated shooting function, the associated strategy and the homotopic parameter.

5. NUMERICAL RESULTS

L_m	R_m	K_m	V_{alim}	r	K_r	g	K_f	M	ρ	S	C_x	R_{bat}
0.05	0.03	0.27	150.0	0.33	10.0	9.81	0.03	250.0	1.293	2.0	0.4	0.05

TABLE 3. Names and values of the electric solar car parameters.

5.1. Case study

In the following subsections, we present the numerical results we obtained for different instances of problem (P_{tmin}). From the experimental point of view we are interested in parameter values which are real world data, and we choose to model an electrical solar car. These values are taken from [26] and given in Table 3. The different instances of problem (P_{tmin}) depend on the values of $i_{\max}$ and $v_{\max}$. The parameter α_f will be fixed to 100. In this setting, the state unconstrained problem is quite simple since the optimal trajectory is γ_+, see proposition 2.11. The complexity comes from the two state constraints of orders 1 and 2. Different phenomenons are expected depending on which constraint is active. Let consider first an homotopy on the bound of an order 1 state constraint, let's say $i_{\max}$. For big enough values of $i_{\max}$, the optimal trajectory has no contact point nor boundary arc. It is known that if we start to decrease the value of $i_{\max}$ until we get a trajectory with a contact point, then for values of $i_{\max}$ just smaller, the contact point is turned into a boundary arc of small length. This is quite different for an order 2 state constraint. We start again with a big value of $v_{\max}$ and then we decrease $v_{\max}$ until we have a trajectory with a contact point. Then, for just smaller values of $v_{\max}$, we still have trajectories with only a contact point and not a boundary arc. This can be seen in subsection 5.3. Some examples with state constraints of different orders are solved (analytically) in Bryson *et al.* [9] and Jacobson *et al.* [17].

5.2. Procedure to study the influence of $i_{\max}$ and $v_{\max}$ on BC-extremals

We start this section with a remark which is crucial for the numerical experiments of section 5.

Remark 5.1. Actually, from any zero of any shooting function is associated a unique 4-tuple $(x(\cdot), p(\cdot), u(\cdot), \eta(\cdot))$ which is not necessarily a BC-extremal. The shooting method does not guarantee that the state $x(\cdot)$ satisfies the path constraints and that the times are well ordered. Indeed, solving for example $S_2 = 0$ could give a time t_2 smaller than the time t_1. Hence, when we solve the shooting equations, we have to check a posteriori that the associated 4-tuple is a BC-extremal. To guarantee that the 4-tuple is a BC-extremal we check that $c_1(x(t)) \leq 0$ and $c_3(x(t)) \leq 0$ for all $t \in [t_0\,, t_f]$, and we check that $t_i \leq t_{i+1}$, where t_i is either the initial time or the final time or a switching time.

Definition 5.2. We say that the 4-tuple associated to a zero of a shooting function is *admissible* if it is a BC-extremal and *non admissible* if it is not a BC-extremal. We say that a structure is *admissible* if it exists a zero of the associated shooting function for which the associated 4-tuple is admissible, and we say that a structure is *non admissible* in the other case.

The procedure to study the influence of $i_{\max}$ and $v_{\max}$ on the structure of the BC-extremals is the following:

(1) The maximum principle combined with geometric analysis is applied first to reduce the set of possible types of extremals, then to compute the parameterization of each kind of possible extremals (*i.e.* it gives the analytical expressions of the control and the Lagrange multiplier η), and finally to give junction conditions.
(2) For a given admissible structure, in order to apply indirect numerical methods, we need first to define the associated shooting function, and then the shooting function is computed, and its regularity and invertibility are checked.
(3) All the study is about how the structures evolve with respect to the parameters $i_{\max}$ and $v_{\max}$. Hence, we fix starting values for $i_{\max}$ and $v_{\max}$, and we fix an initial admissible structure. In our case, we fix $i_{\max}$ and $v_{\max}$ big enough such that γ_+ is admissible (it is even the optimal structure, see proposition 2.11).
(4) Numerical simulations based on indirect methods are applied; starting from a BC-extremal given by the shooting methods, we use homotopy methods to deform the BC-extremal until we detect[5] that the associated 4-tuple becomes non admissible.

[5]With the `HamPath` code, we can check if the structure is admissible at each integration step of the homotopy method, and we can stop the homotopy if a change in the structure occurs.

(5) When we detect along an homotopy that the 4-tuple is non admissible, we determine the new structure combining the theoretical results with the reason for the change in the structure and then we look for a new adimissible 4-tuple. Let note $\Lambda \coloneqq (i_{\max}, v_{\max})$ the value when the structure has to change. Before starting a new homotopy we valid the new structure by checking first that this new structure is admissible and then by checking that the limit cases for both structures (the old and the new) at Λ give the same trajectory.

Remark 5.3. In this procedure, we do not check the global optimality of the BC-extremals but only the fact that the structures are valid, *i.e.* admissible and have compatible limit cases.

This procedure is exactly the method we use in section 5.3. To explain in detail the construction of the synthesis in section 5.4, we need the following definition about the degree of an admissible structure at a given point $\Lambda \coloneqq (i_{\max}, v_{\max})$.

Definition 5.4. We say that a structure γ is of *degree 1 at* $\bar{\Lambda}$ if it exists a neighborhood $\mathcal{V} \subset \mathbb{R}^2$ of $\bar{\Lambda}$ such that for every $\Lambda \in \mathcal{V}$, γ is admissible at Λ (*i.e.* when the values of the parameters $i_{\max}$ and $v_{\max}$ are given by Λ). We say that a structure γ is of *degree k at* $\bar{\Lambda}$, $k \geq 2$, if for every sufficiently small neighborhood $\mathcal{V}$ of $\bar{\Lambda}$, there exists k structures γ_i, there exists k sets D_i of non empty interior and a set I of empty interior such that $\{I, D_1, \cdots, D_k\}$ is a partition of $\mathcal{V}$ and such that for every $\Lambda_i \in D_i$, $i = 1, \cdots, k$, γ_i is of degree 1 at Λ_i, and the structures are compatible, *i.e.* the limit cases at a given point of $\mathcal{V}$ give the same trajectory.

Remark 5.5. In the Figure 19 presenting the synthesis, the structures of degree 2 are given by the blue lines, while the structures of degree greater than 3 are represented by red points. The structures of degree 1 are contained in the domains of non-empty interiors.

In section 5.3, to study the practical case when $i_{\max} = 150$, we only perform homotopies on structures of degree 1 and we detect a change when we reach a structure[6] of degree 2. To construct the synthesis with respect to the parameters $i_{\max}$ and $v_{\max}$ we do the following:

(1) We start an homotopy on a structure of degree 1 until we reach a structure of degree 2. We start a new homotopy with the new valid structure of degree 1 and continue the exploration.
(2) We compute the branch (a blue line on Figure 19) corresponding to a structure of degree 2 by homotopy until we reach a structure of degree greater than 3.

We can see that the construction of the synthesis is heuristic and about exploration. Thus, the synthesis represented by the Figures 19 and 20 is not necessarily complete. Moreover, this procedure does not guarantee the optimality of the BC-extremals but this synthesis is a first step toward the optimal synthesis.

5.3. Influence of the maximal current and the maximal velocity (with $\alpha_f = 100$)

From now on, the parameter α_f is fixed to 100, so the car has to cover 100m in minimum time. We are interested in the case $i_{\max} = 150$ since it has a practical interest, see [26]. In this case, the optimal trajectories may have boundary arcs. Thus, we start with values of $i_{\max}$ and $v_{\max}$ big enough to deal with trajectories without boundary arcs. Then we first decrease the value of $i_{\max}$ to $i_{\max} = 150$ and finally we build a sub-optimal synthesis for $i_{\max} = 150$ and $v_{\max} \in [10\,, 110]$. A schematic view of the method is presented in Figure 4, that we explain hereinafter.

- Let fix $(i_{\max}, v_{\max}) = (1100, 110)$. By proposition 2.11 the optimal trajectory is in this case γ_+.
- When $(i_{\max}, v_{\max}) = (i_{\max}^{c_1}, 110)$, the trajectory has now a contact point with the boundary C_1, thus the strategy is $\gamma_+^{c_1}$, $c_1(x) = x_1 - 1$. For $(i_{\max}, v_{\max}) = (i_{\max}^{c_1} - \varepsilon, 110)$, $\varepsilon > 0$ small, the contact point has turned into a boundary arc since the constraint is of order 1. The structure becomes $\gamma_+\gamma_{c_1}\gamma_+$, with $t_1 < t_2$ the junction times with the boundary. According to lemma 3.5, $\nu_1 = 0$ and $\nu_2 < 0$, so the control is continuous at t_2. Moreover, the boundary control $u_{c_1}(\cdot)$ is strictly increasing since $a_4 + a_5 + a_6 > 0$, so it has to be discontinuous at time t_1 and continuous at time t_2 and $\mathbf{A_3}$ is satisfied.

[6] We can consider in this case that the probability to reach a structure of degree greater than 3 is zero.

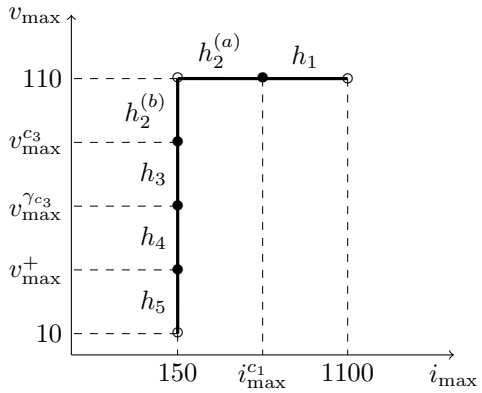

FIGURE 4. Schematic view of the method used to compute the sub-optimal synthesis for $\alpha_f = 100$, $i_{\max} = 150$ and $v_{\max} \in [10\,, 110]$, starting from $(i_{\max}, v_{\max}) = (1100, 110)$. The symbol $\bullet$ represents a change of structure while $\circ$ means a choice to start or stop an homotopy. The scale is not respected. See Table 2 for the corresponding structures.

- When $(i_{\max}, v_{\max}) = (150, v_{\max}^{c_3})$, the last arc has a contact point with the boundary C_3 ($c_3(x) = x_3 - 1$). For just smaller values of $v_{\max}$, *i.e.* for $v_{\max} = v_{\max}^{c_3} - \varepsilon$, $\varepsilon > 0$ small, the structure has to change. Indeed, the last bang arc would cross the boundary, so this arc becomes a sequence $\gamma_+\gamma_-\gamma_+$ (there is no singular arc, see proposition 2.5). It is quite different from previous item, since here the constraint is of order 2; the trajectory for $v_{\max} = v_{\max}^{c_3} - \varepsilon$ still has a contact point with C_3. As a consequence, the limit case for $v_{\max} = v_{\max}^{c_3}$ is not $\gamma_+\gamma_{c_1}\gamma_+^{c_3}$ but $\gamma_+\gamma_{c_1}\gamma_+^{H_1,c_3}$ and the last bang arc has a contact of order 2 with the switching surface.
- When $(i_{\max}, v_{\max}) = (150, v_{\max}^{\gamma_{c_3}})$, the boundary control $u_{c_3}(\cdot)$ is admissible, *i.e.* $u_{c_3}(\cdot) = 1$, which gives $v_{\max}^{\gamma_{c_3}} \approx 65.6042$. The structure for $v_{\max} = v_{\max}^{\gamma_{c_3}} - \varepsilon$ is $\gamma_+\gamma_{c_1}\gamma_+\gamma_-\gamma_{c_3}$.
- When $(i_{\max}, v_{\max}) = (150, v_{\max}^{+})$ the second bang arc collapses, and the trajectories become $\gamma_+\gamma_{c_1}\gamma_-\gamma_{c_3}$.

5.3.1. *Homotopies h_1 and $h_2^{(a)}$ and intermediate trajectory of the form $\gamma_+^{c_1}$*

We first choose $i_{\max}$ and $v_{\max}$ big enough to get a trajectory with only interior arcs. In this case, the optimal trajectory is of the form γ_+. We fix $i_{\max} = 1100$A and $v_{\max} = 110$km.h^{-1} and we solve $S_1(y_1) = 0$, where $y_1 \coloneqq (p_0, t_f)$. The solution is $\bar{y}_1 \approx (0.3615, 6.4479, 0.2416, 5.6156)$[7]. The trajectory $x(\cdot)$ with its associated costate $p(\cdot)$ are portrayed in Figure 5. Let $i_{\max}^{c_1} = i_{\max} \times \max_{t\in[0,t_f]} x_1(t) \approx 1081.94$, $i_{\max} = 1100$, denote the maximal current along the trajectory $x(\cdot)$. This maximal current does not depend on $i_{\max}$ for the trajectories of the form γ_+. For $(i_{\max}, v_{\max}) = (i_{\max}^{c_1}, 110)$, then the structure is $\gamma_+^{c_1}$. We use the differential homotopy method presented in section 4.3 to solve $h_1(y_1, i_{\max}) = 0$, for $i_{\max} \in [i_{\max}^{c_1}\,, 1100]$, starting from $i_{\max} = 1100$.

When $i_{\max} < i_{\max}^{c_1}$ the structure is $\gamma_+\gamma_{c_1}\gamma_+$. To initialize the shooting method and solve $S_2(y_2) = 0$, $y_2 \coloneqq (p_0, t_f, t_1, t_2, \nu_2, z_1, z_2)$, we use the BC-extremal γ_+ with $i_{\max} = i_{\max}^{c_1}$ from the path of zeros of h_1. Then we solve $h_2^{(a)}(y_2, i_{\max}) = 0$, for $i_{\max} \in [150\,, i_{\max}^{c_1}]$, starting from $i_{\max} = i_{\max}^{c_1}$. Figure 6 displays the initial, the junction and the final times and the jump ν_2 along the path of zeros of $h_2^{(a)}$. One may notice that the jump is not zero when $i_{\max} = i_{\max}^{c_1}$. As a consequence, the extremals at $i_{\max} = i_{\max}^{c_1}$ from the paths of zeros of h_1 and $h_2^{(a)}$ are not equal. The state trajectories are the same but not the costate trajectories. However, the differences between the costates are clearly shown in Figure 7. As a matter of fact, from the solution $(\bar{y}_1, i_{\max}^{c_1})$ of $h_1(y_1, i_{\max}^{c_1}) = 0$, it is possible to determine completely the solution $(\bar{y}_2, i_{\max}^{c_1})$ of $h_2^{(a)}(y_2, i_{\max}^{c_1}) = 0$, and we can easily initialize the homotopy $h_2^{(a)}$.

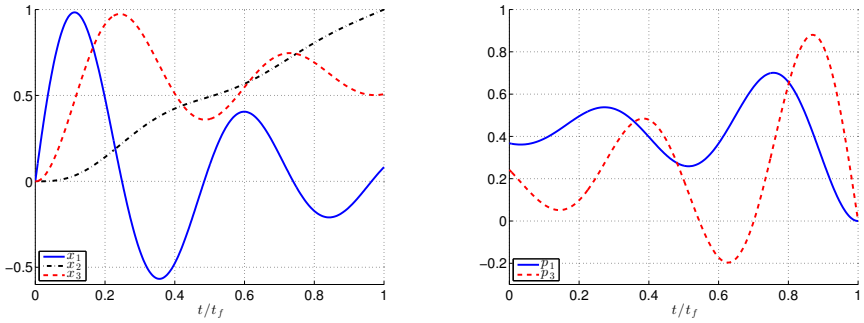

FIGURE 5. **Trajectory** γ_+. State and costate for $(i_{\max}, v_{\max}) = (1100, 110)$. The component $p_2 \approx 6.4479$ is constant. The terminal constraint $x_2(t_f) = 1$ is satisfied.

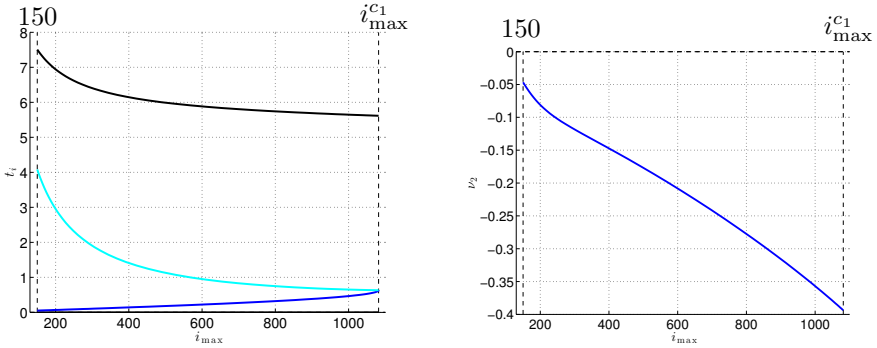

FIGURE 6. **Homotopy** $h_2^{(a)}$. (Left) The initial, the junction and the final times along the path of zeros of $h_2^{(a)}$. The junction times collapse at $i_{\max} = i^{c_1}_{\max}$. The length of the boundary arc increases as $i_{\max}$ decreases. (Right) The jump $\nu_2 \le 0$ along the path.

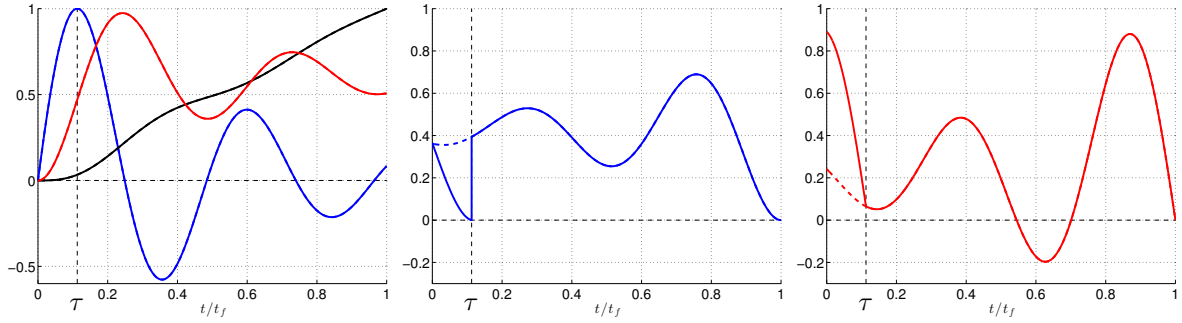

FIGURE 7. **Trajectories** $\gamma_+^{c_1}$. The BC-extremal of the form $\gamma_+^{c_1}$ at $i_{\max} = i^{c_1}_{\max}$ from h_1 is represented by dashed lines while the one from $h_2^{(a)}$ is represented by solid lines. The contact with the boundary is at time $\tau = t_1 = t_2$, where t_1, t_2 are the junction times of trajectories $\gamma_+\gamma_{c_1}\gamma_+$. (Left) The state trajectories (compare with Figure 5). (Middle) $p_1(\cdot)$. (Right) $p_3(\cdot)$. The trajectories are identical while the adjoint vectors are similar only after τ.

[7]The value of $\bar{y}_1$ with all the digits gives a very accurate solution since $\|S_1(\bar{y}_1)\| \approx 1.5e^{-15}$.

5.3.2. *Homotopies $h_2^{(b)}$ and h_3 and intermediate trajectory of the form $\gamma_+\gamma_{c_1}\gamma_+^{H_1,c_3}$*

Up to this point, we have a trajectory $\gamma_+\gamma_{c_1}\gamma_+$ for $(i_{\max}, v_{\max}) = (150, 110)$. Now we start to decrease the value of $v_{\max}$ to obtain all the trajectories for $i_{\max} = 150$. We start by computing the path of zeros of $h_2^{(b)}$ until we reach $v_{\max} = v_{\max}^{c_3}$, for which the associated trajectory has a contact point with the boundary C_3. Let $x(\cdot)$ denote the trajectory of the form $\gamma_+\gamma_{c_1}\gamma_+$ for $(i_{\max}, v_{\max}) = (150, 110)$. Then the maximal speed is given by $v_{\max}^{c_3} = v_{\max} \times \max_{t\in[0,t_f]} x_3(t) \approx 70.3716$, $v_{\max} = 110$, and it does not depend on $v_{\max}$ for the trajectories of the form $\gamma_+\gamma_{c_1}\gamma_+$, for which $i_{\max} = 150$ is fixed. For $(i_{\max}, v_{\max}) = (150, v_{\max}^{c_3})$, then the structure is $\gamma_+\gamma_{c_1}\gamma_+^{H_1,c_3}$. We solve $h_2^{(b)}(y_2, v_{\max})$, for $v_{\max} \in [v_{\max}^{c_3}, 110]$, starting from $v_{\max} = 110$. Along the path of zeros of $h_2^{(b)}$ the initial, the junction and the final times, and the jump ν_2 are constant. When $v_{\max} < v_{\max}^{c_3}$ the structure is $\gamma_+\gamma_{c_1}\gamma_+\gamma_-\gamma_+^{c_3}$. We fix now $v_{\max} = v_{\max}^{c_3}$, and $i_{\max} = 150$. To initialize the shooting method and solve $S_3(y_3) = 0$, $y_3 := (p_0, t_f, t_1, t_2, \nu_2, t_3, t_4, t_5, \nu_5, z_1, z_2, z_3, z_4, z_5)$, we use the BC-extremal $\gamma_+\gamma_{c_1}\gamma_+$ at $v_{\max} = v_{\max}^{c_3}$ from the path of zeros of $h_2^{(b)}$. Then we solve $h_3(y_3, v_{\max}) = 0$ for $v_{\max} \in [v_{\max}^{\gamma_{c_3}}, v_{\max}^{c_3}]$, starting from $v_{\max} = v_{\max}^{c_3}$ and with $v_{\max}^{\gamma_{c_3}} \approx 65.6042$. Figure 8 shows the initial, the switching, the junction and the final times along the path of zeros of h_3, while the jumps ν_2 and ν_5 are portrayed in Figure 9. Figure 10 gives details about the limit case when $v_{\max} = v_{\max}^{c_3}$.

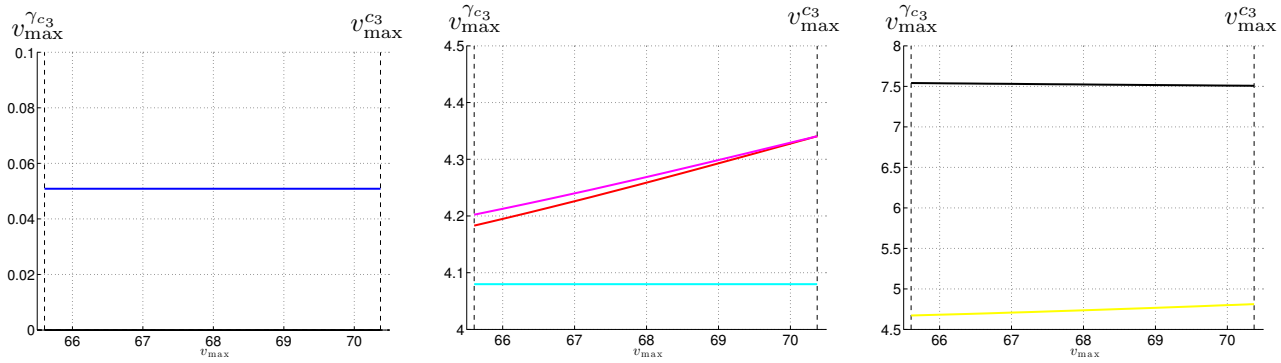

FIGURE 8. **Homotopy** h_3. The initial, the switching, the junction and the final times along the path of zeros of h_3. (Left) The times $t_0 \equiv 0$ and t_1. (Middle) The times t_2, t_3 and t_4. (Right) The times t_5 and t_f. The length $t_2 - t_1$ of γ_{c_1} is constant while the length of γ_- vanishes when $v_{\max} = v_{\max}^{c_3}$, *i.e.* when the trajectory is of the form $\gamma_+\gamma_{c_1}\gamma_+^{H_1,c_3}$.

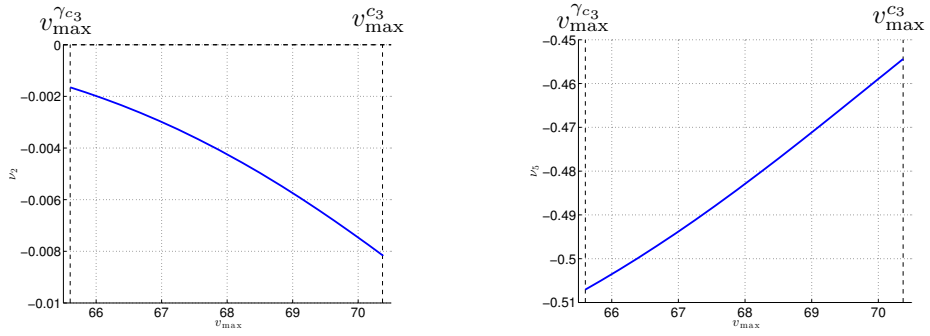

FIGURE 9. **Homotopy** h_3. The jumps $\nu_2 \leq 0$ (left) and $\nu_5 \leq 0$ (right) along the path of zeros of h_3.

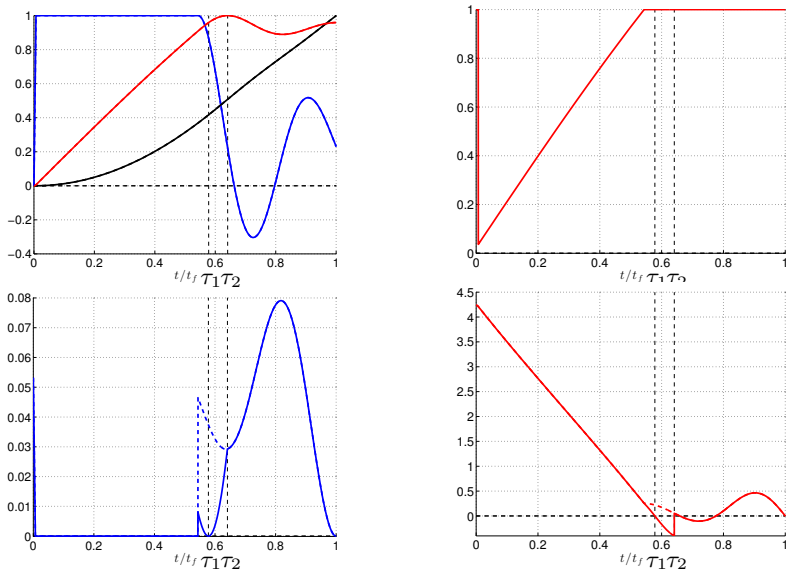

FIGURE 10. **Trajectories $\gamma_+\gamma_{c_1}\gamma_+^{c_3}$ and $\gamma_+\gamma_{c_1}\gamma_+^{H_1,c_3}$.** The BC-extremal $\gamma_+\gamma_{c_1}\gamma_+^{c_3}$ at $v_{\max} = v_{\max}^{c_3}$ from $h_2^{(b)}$ is represented by dashed lines while the one $\gamma_+\gamma_{c_1}\gamma_+^{H_1,c_3}$ from h_3 is represented by solid lines. The contact with the boundary C_3 is at time τ_2, while the contact of order 2 with Σ_1^0 is at time $\tau_1 < \tau_2$. (Top-Left) The state trajectories (compare with Figure 5). (Top-Right) The control. (Bottom-Left) The component $p_1(\cdot)$. (Bottom-Right) The component $p_3(\cdot)$.

5.3.3. *Homotopy h_4 and intermediate case $\gamma_+\gamma_{c_1}\gamma_+\gamma_-\gamma_{c_3}$, with $u_{c_3}(\cdot) \equiv +1$, between h_3 and h_4*

The BC-extremal at $v_{\max} = v_{\max}^{\gamma_{c_3}}$ from h_3 is $\gamma_+\gamma_{c_1}\gamma_+\gamma_-\gamma_+^{c_3}$ with $c_3(\cdot) \equiv 0$ along the last bang arc. For this specific value of $v_{\max}$, the boundary control u_{c_3} is admissible if we replace the last bang arc by an arc γ_{c_3}. For $v_{\max} = v_{\max}^{\gamma_{c_3}} - \varepsilon$, $\varepsilon > 0$ small, the trajectory becomes $\gamma_+\gamma_{c_1}\gamma_+\gamma_-\gamma_{c_3}$ and the boundary control along the arc γ_{c_3} is strictly admissible, *i.e.* assumption $\mathbf{A_3}$ holds. Here again, we use the last solution from h_3 to initialize and solve $S_4(y_4) = 0$, $y_4 := (p_0, t_f, t_1, t_2, \nu_2, t_3, t_4, \nu_4, z_1, z_2, z_3, z_4)$, with $v_{\max} = v_{\max}^{\gamma_{c_3}}$. Then we solve $h_4(y_4, v_{\max}) = 0$ for $v_{\max} \in [v_{\max}^+, v_{\max}^{\gamma_{c_3}}]$ starting from $v_{\max} = v_{\max}^{\gamma_{c_3}}$. The homotopy process has to stop when $t_2 \geq t_3$ (or $\nu_2 \geq 0$), which gives $v_{\max}^+ \approx 64.1641$. Figure 11 shows the initial, the switching, the junction and the final times along the path of zeros of h_4, while the jumps ν_2 and ν_4 are portrayed in Figure 12. Figure 13 gives details about the limit case when $v_{\max} = v_{\max}^+$.

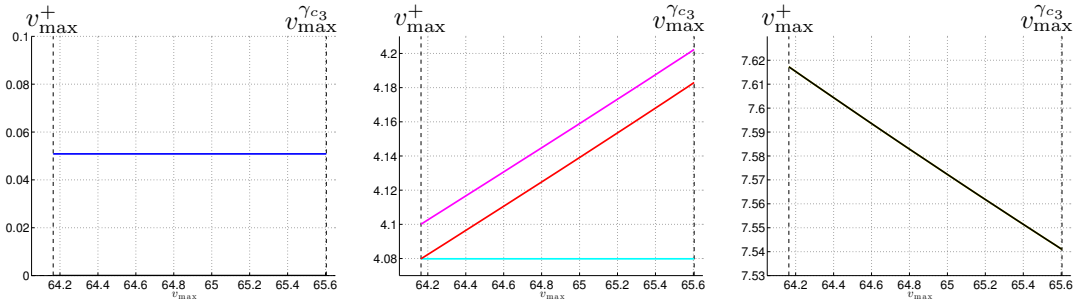

FIGURE 11. **Homotopy h_4.** The initial, the switching, the junction and the final times along the path of zeros of h_4. (Left) The times $t_0 \equiv 0$ and t_1. (Middle) The times t_2, t_3 and t_4. (Right) The final time t_f. The length $t_3 - t_2$ vanishes when $v_{\max} = v_{\max}^+$.

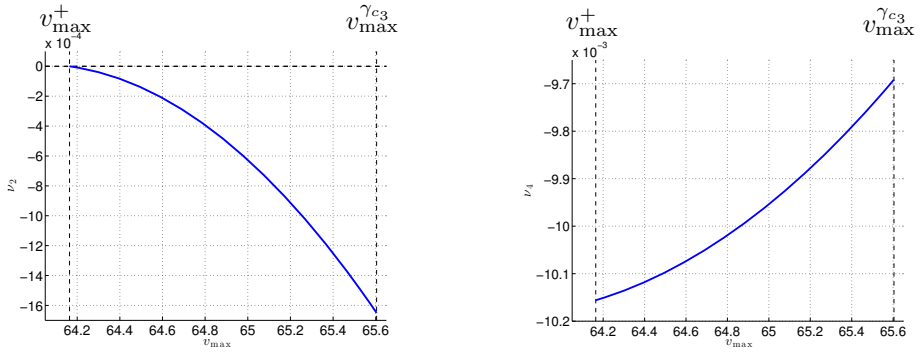

FIGURE 12. **Homotopy** h_4. The jumps $\nu_2 \leq 0$ (left) and $\nu_4 \leq 0$ (right) along the path of zeros of h_3. Note that the jump ν_2 vanishes when $v_{\max} = v^+_{\max}$, see lemma 3.5. The jump $\nu_4 < 0$ according to lemma 3.8.

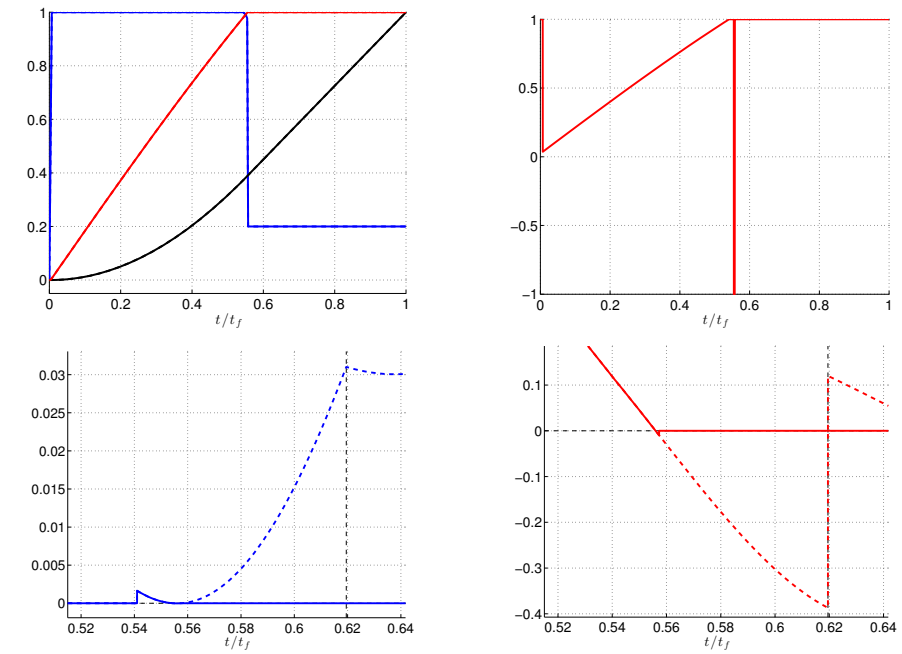

FIGURE 13. **Trajectories** $\gamma_+\gamma_{c_1}\gamma_+\gamma_-\gamma_+^{c_3}$ **and** $\gamma_+\gamma_{c_1}\gamma_+\gamma_-\gamma_{c_3}$**, with** $u_{c_3}(\cdot) = +1$. The BC-extremal $\gamma_+\gamma_{c_1}\gamma_+\gamma_-\gamma_+^{c_3}$ at $v_{\max} = v^{\gamma_{c_3}}_{\max}$ from h_3 is represented by dashed lines while the one $\gamma_+\gamma_{c_1}\gamma_+\gamma_-\gamma_{c_3}$ from h_4 is represented by solid lines. (Top-Left) The state trajectories. (Top-Right) The control. (Bottom-Left) Zoom on the component $p_1(\cdot)$. (Bottom-Right) Zoom on the component $p_3(\cdot)$. About the trajectory $\gamma_+\gamma_{c_1}\gamma_+\gamma_-\gamma_{c_3}$ with $u_{c_3}(\cdot) = +1$, the components $p_1(\cdot)$ and $p_3(\cdot)$ are identically zero along γ_{c_3} since this extremal is a limit case from h_4 for which for each solution, the functions Φ and $\dot{\Phi}$ are zero along γ_{c_3}. Note that the sine wave shapes of the trajectory at Figure 7 have changed into square wave shapes.

5.3.4. *Homotopy h_5 and intermediate case $\gamma_+\gamma_{c_1}\gamma_+\gamma_-\gamma_{c_3}$, with $t_2 = t_3$, between h_4 and h_5*

Here is the last homotopy. We use the solution from h_4 at $v_{\max} = v^+_{\max}$ to initialize and solve $S_5(y_5) = 0$, $y_5 := (p_0, t_f, t_1, t_2, t_3, \nu_3, z_1, z_2, z_3)$. This is done easily since t_3, ν_3 and z_3 are given respectively by t_4, ν_4 and z_4 from the solution from h_4. In other words, at $v_{\max} = v^+_{\max}$, the extremals are the same from both the solutions from h_4 and h_5. This is new compare to the others homotopies[8], for which the limit cases have different adjoint vectors. Figures 16 and 17 only shows the components $p_1(\cdot)$ and $p_3(\cdot)$ of the extremal for $v_{\max} = v^+_{\max}$ since the trajectory is quite similar from the one in Figure 13 and the shape of the control can be guessed from Figure 13. Figure 14 shows the initial, the junction and the final times along the path of zeros of h_5, while the jumps ν_3 and the length $t_3 - t_2$ of the arc γ_- are portrayed in Figure 15. One may note that the final time has not a linear shape with respect to $v_{\max}$. It increases more and more when $v_{\max}$ decreases, contrary to the length of the boundary arc γ_{c_1} which decreases linearly. Besides, the length of γ_- is small but not constant.

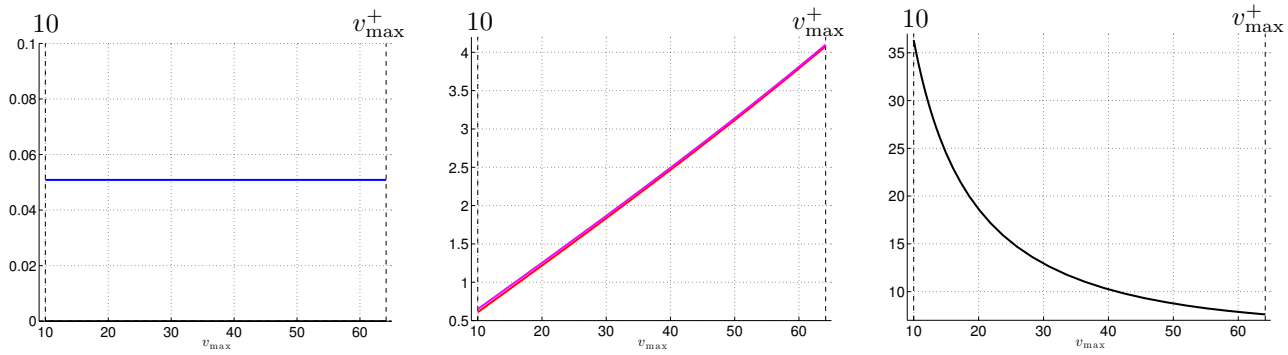

FIGURE 14. **Homotopy h_5.** The initial, the junction and the final times along the path of zeros of h_5. (Left) The times $t_0 \equiv 0$ and t_1. (Middle) The times t_2, t_3. (Right) The final time t_f. The length $t_3 - t_2$ is small but not constant, see Figure 15. The length of the first bang arc is still constant.

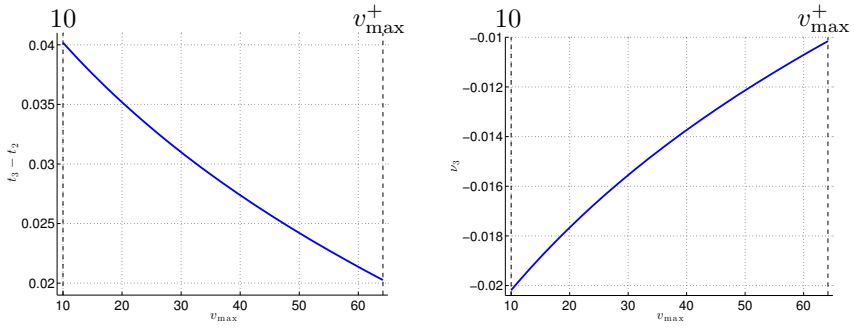

FIGURE 15. **Homotopy h_5.** The length $t_3 - t_2$ (left) and the jump ν_3 (right) along h_5.

[8]Except obviously between $h_2^{(a)}$ and $h_2^{(b)}$.

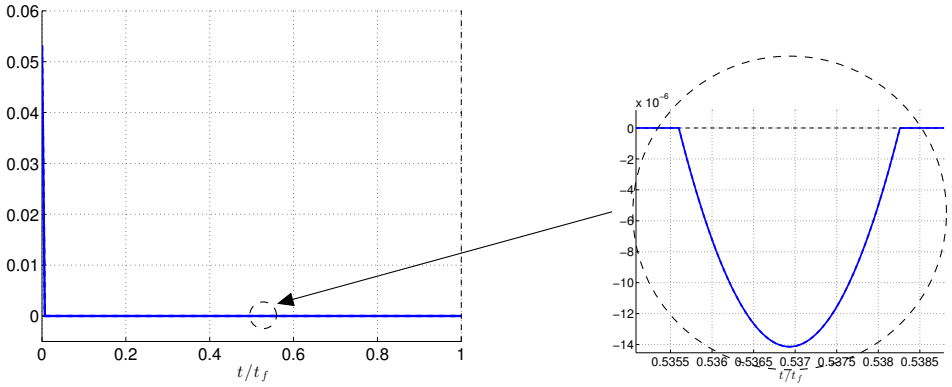

FIGURE 16. **Trajectory $\gamma_+\gamma_{c_1}\gamma_+\gamma_-\gamma_{c_3}$, with $t_2 = t_3$.** The BC-extremal $\gamma_+\gamma_{c_1}\gamma_+\gamma_-\gamma_{c_3}$ with $t_2 = t_3$ is the same as the BC-extremal $\gamma_+\gamma_{c_1}\gamma_-\gamma_{c_3}$ from h_5 at $v_{\max} = v^+_{\max}$. (Left) The component $p_1(\cdot)$ with a zoom (Right) around γ_-. $p_1(\cdot)$ is zero along γ_{c_1} and γ_{c_3}.

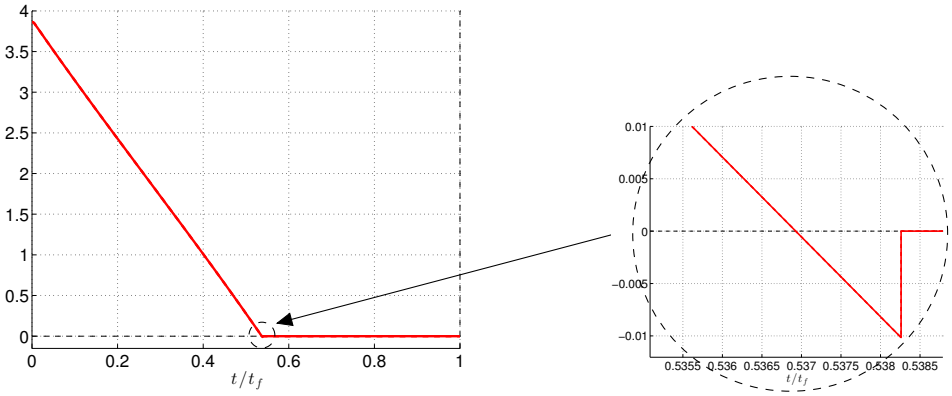

FIGURE 17. **Trajectory $\gamma_+\gamma_{c_1}\gamma_+\gamma_-\gamma_{c_3}$, with $t_2 = t_3$.** The BC-extremal $\gamma_+\gamma_{c_1}\gamma_+\gamma_-\gamma_{c_3}$ with $t_2 = t_3$ is the same as the BC-extremal $\gamma_+\gamma_{c_1}\gamma_-\gamma_{c_3}$ from h_5 at $v_{\max} = v^+_{\max}$. (Left) The component $p_3(\cdot)$ with a zoom (Right) around γ_-. The component $p_3(\cdot)$ is zero only along γ_{c_3}.

5.3.5. *Norm of homotopic functions along the paths of zeros for* $v_{\max} \in [10\,, 110]$

Finding zeros of shooting functions (or homotopic functions) guarantees the complete characterization of the associated BC-extremals. We represent on Figure 18 the norm along the paths of zeros of the following homotopic functions: h_5, h_4, h_3 and $h_2^{(b)}$, respectively for $v_{\max}$ in $[10\,, v^+_{\max}]$, $[v^+_{\max}\,, v^{\gamma_{c_3}}_{\max}]$, $[v^{\gamma_{c_3}}_{\max}\,, v^{c_3}_{\max}]$ and $[v^{c_3}_{\max}\,, 110]$. At the end of each homotopy we perform a correction using the shooting methods which explains the discontinuities at $v^+_{\max}$, $v^{\gamma_{c_3}}_{\max}$ and $v^{c_3}_{\max}$. We can see that the corrections give very accurate solutions while along the homotopies, the norm increases quickly before reaching asymptotic values. We can notice two different behaviours. Along $h_5^{-1}(0)$, the asymptotic value is around $2e^{-9}$ which is consistent with the tolerances of $1e^{-10}$ given to the Runge-Kutta method (`dopri5`). Along the other homotopies, the asymptotic value is greater but around $4e^{-5}$ which is accurate enough.

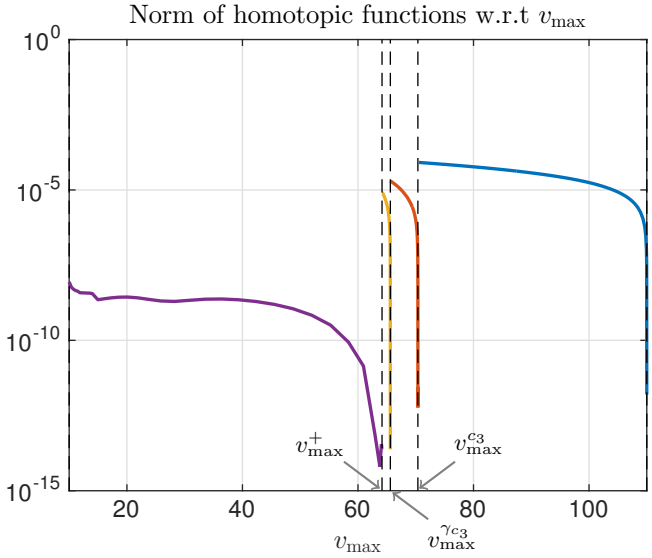

FIGURE 18. Norm along the paths of zeros of the following homotopic functions: h_5, h_4, h_3 and $h_2^{(b)}$, respectively for $v_{\max}$ in $[10\,, v_{\max}^{+}]$, $[v_{\max}^{+}\,, v_{\max}^{\gamma_{c_3}}]$, $[v_{\max}^{\gamma_{c_3}}\,, v_{\max}^{c_3}]$ and $[v_{\max}^{c_3}\,, 110]$.

5.4. **Synthesis with respect to $i_{\max}$ and $v_{\max}$**

We present in Figure 19 the best sub-optimal synthesis we obtain using all the techniques and results established throughout this paper. See section 5.2 for the procedure to construct this sub-optimal synthesis. We also need the proposition 5.6 to get the results presented in Figure 20. We make this synthesis for $i_{\max} \geq 10$, $v_{\max} \geq 10$ and $\alpha_f = 100$.

Proposition 5.6. *Let consider a boundary arc γ_{c_1} defined on $[t_1\,, t_2]$ with $(z(\cdot), u_{c_1}(\cdot), \eta_{c_1}(\cdot))$ its associated extremal. Let assume there exists $\tau \in [t_1\,, t_2]$ such that $H_1(z(\tau)) = H_{01}(z(\tau)) = 0$ and that $\mathbf{A_3}$ holds along γ_1. Then either $\tau = t_1$ or $\tau = t_2$.*

Proof. Let assume $\tau \in (t_1\,, t_2)$. Along γ_{c_1}, $\eta_{c_1} = H_{01}/(F_1 \cdot c_1) \leq 0$ with $F_1 \cdot c_1 \equiv a_7 > 0$, so $H_{01} \leq 0$. At time τ, $H_{01}(z(\tau)) = 0$ and $\dot{H}_{01}(z(\tau)) = H_{001}(z(\tau)) - \eta_{c_1}(z(\tau))(F_{01} \cdot c_1)(x(\tau)) = H_{001}(z(\tau)) \neq 0$, since $\dim \mathrm{Span}(F_1(x(\tau)), F_{01}(x(\tau)), F_{001}(x(\tau))) = 3$ and $p(\tau) \neq 0$. As a consequence, the sign of H_{01} changes when crossing $t = \tau$, which is not possible. □

Remark 5.7. To build this synthesis we do not deal with the possible local minima since the aim of this paper is not to prove the global optimality of the synthesis but to describe how we can build it starting from one point, *i.e.* one BC-extremal for a given value of $(i_{\max}, v_{\max})$. Here we start from the optimal trajectory γ_+. To construct this synthesis we catch the changes along the homotopies and determine the new strategy using the theoretical results. However, if we consider a general optimal control problem depending on a parameter λ, then to get a better synthesis, for a given $\overline{\lambda}$ we should compare the cost associated to each component of $h^{-1}(\{0\}) \cap \{\lambda = \overline{\lambda}\}$, for each homotopic function h. This approach is crucial when the optimal control problem has for example many local solutions, see [6].

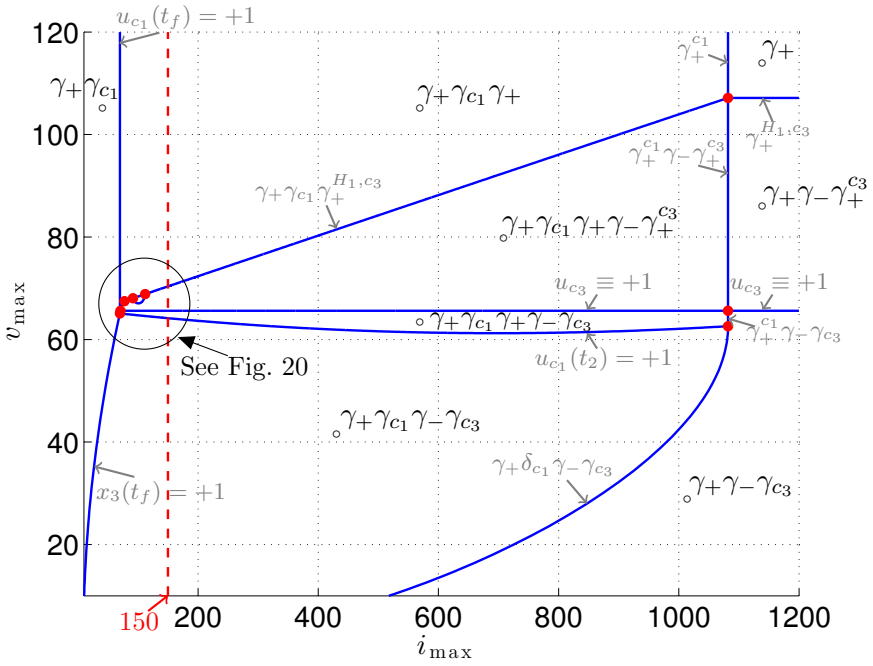

FIGURE 19. **Synthesis with respect to $i_{\max}$ and $v_{\max}$.** The structures are displayed on the graph. The sequence labeled $\gamma_+\delta_{c_1}\gamma_-$ means that there is a contact point with the constraint set C_1 at the switching time between γ_+ and γ_-. The blue lines represent structures of degree 2 while at the red points we have structures of degree 3 or 4.

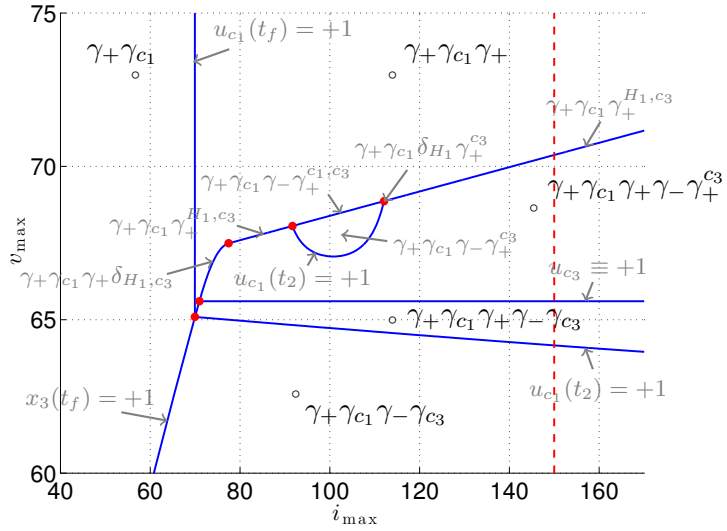

FIGURE 20. **Zoom of the synthesis**. The structures are displayed on the graph. The sequence labeled $\gamma_{c_1}\delta_{H_1}$ means that there is a contact point of order 2 with the switching surface at the exit-time of the boundary arc.

6. Conclusion

In this paper, we have presented the minimum time control problem of an electric vehicle which have been modeled as a Mayer problem in optimal control, with affine dynamics with respect to the control (scalar) and with two state constraints, one of order 1 and the other of order 2, see sections 1.2 and 3.3.3. We have tackled first the state unconstrained problem from the application of the Pontryagin Maximum Principle, see section 2.1, which gives necessary conditions of optimality. Then we used in section 2.2 the Lie bracket configuration to show that the only existing extremals are bang-bang with finitely many switchings (see section 2.3) and we proved in 2.5 that the optimal trajectory is of the form γ_+. Nevertheless, the classification of bang-bang extremals, presented in section 2.4, was an efficient tool to describe the behavior of some possible extremals (here for the state constrained case) and to get better insight into such extremals, see section 5.3.2. The analysis of problem (P_{tmin}), *i.e.* with the state constraints, consisted first in computing the boundary controls and the multipliers associated to the state constraints, for both the first and second-order constraints. On the other hand, we gave new junction conditions, see section 3.3, which have been used to define multiple shooting functions in sections 4.2.1 and 4.2.3. Moreover, we gave a local time minimal synthesis, see section 3.4, that we encountered in the numerical simulations in sections 5.3.3 and 5.3.4. Finally, in section 5.4, we obtained a synthesis of solutions which satisfy the necessary conditions of optimality (*i.e.* BC-extremals) with respect to the parameters $i_{\max}$ and $v_{\max}$, with $x_1(0)$, $x_3(0)$, α_f fixed, and for one specific car.

The same techniques could be applied to other problems, such as the problem of the minimization of the electric energy (P_{emin}). In this case, the final time t_f is fixed and the structure of the optimal trajectories depends on t_f, see Figure 21. The dynamics associated to problem (P_{emin}) is bilinear on the state and the control variables and this leads to more complex optimal structures with singular extremals. Even though the state unconstrained problem (P_{emin}) is more complex than the time minimal case, the same tools such as Lie bracket configuration and local classification can be used. The main difference comes from the fact that the final time is now a parameter and one may study its influence on the optimal trajectories. This was already done in [6], where a state unconstrained and affine scalar control problem of Mayer form was analyzed taking into account the influence of the final time. Moreover, the state constrained case should be clarified with the same tools as those presented in this paper.

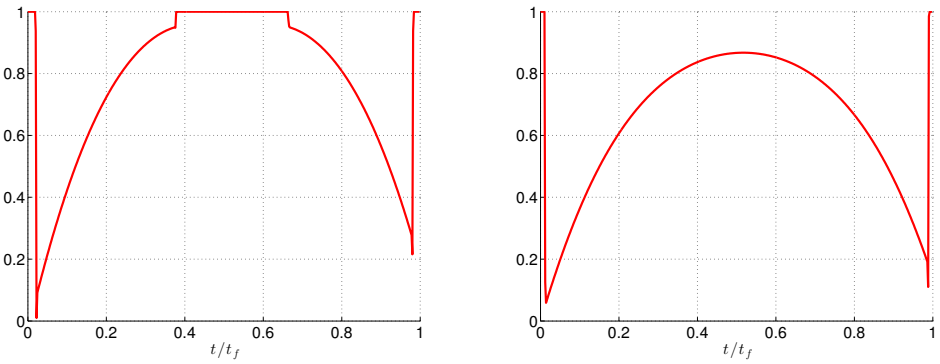

Figure 21. **Problem** (P_{emin}). Optimal control for problem (P_{emin}) for $t_f = 1.25\,T_{\min}$ (left) and $t_f = 1.50\,T_{\min}$ (right), with $T_{\min} \approx 5.6156$, $\alpha_f = 100$, $i_{\max} = 1100$ and $v_{\max} = 110$. The structure is $\gamma_+\gamma_s\gamma_+\gamma_s\gamma_+$ for $t_f = 1.25\,T_{\min}$ and $\gamma_+\gamma_s\gamma_+$ for $t_f = 1.50\,T_{\min}$. The solutions have been computed with the `Bocop` [4] software.

References

[1] A. A. Agrachev & Y. L. Sachkov, *Control theory from the geometric viewpoint*, vol **87** of *Encyclopaedia of Mathematical Sciences*, Springer-Verlag, Berlin (2004), xiv+412.

[2] E. Allgower & K. Georg, *Introduction to numerical continuation methods*, vol. **45** of *Classics in Applied Mathematics*, Soc. for Industrial and Applied Math., Philadelphia, PA, USA, (2003), xxvi+388.

[3] V. G. Boltyanskiĭ, R. V. Gamkrelidze, E. F. Mishchenko, & L. S. Pontryagin, *The mathematical theory of optimal processes*. Classics of Soviet Mathematics. Gordon & Breach Science Publishers, New York, (1986), xxiv+360.

[4] F. J. Bonnans, P. Martinon & V. Grélard. *Bocop - A collection of examples*, Technical report, INRIA, 2012. RR-8053.

[5] B. Bonnard & M. Chyba, *Singular trajectories and their role in control theory*, vol **40** of *Mathematics & Applications*, Springer-Verlag, Berlin (2003), xvi+357.

[6] B. Bonnard, M. Claeys, O. Cots & P. Martinon, *Geometric and numerical methods in the contrast imaging problem in nuclear magnetic resonance*, Acta Appl. Math., **135** (2014), no. 1, 5–45.

[7] B. Bonnard & O. Cots, *Geometric numerical methods and results in the control imaging problem in nuclear magnetic resonance*, Math. Models Methods Appl. Sci., **24** (2012), no. 1, 187–212.

[8] B. Bonnard, L. Faubourg, G. Launay & E. Trélat, *Optimal Control With State Constraints And The Space Shuttle Re-entry Problem*, J. Dyn. Control Syst., **9** (2003), no. 2, 155–199.

[9] A. E. Bryson, W. F. Denham & S.E. Dreyfus, *Optimal programming problems with inequality constraints I: necessary conditions for extremal solutions.*, AIAA Journal, **1** (1963), no. 11, 2544–2550.

[10] R. Bulirsch & J. Stoer, *Introduction to numerical analysis*, vol. **12** of *Texts in Applied Mathematics*, Springer-Verlag, New York, 2^{nd} edition, 1993, xvi+744.

[11] J.-B. Caillau, O. Cots & J. Gergaud, *Differential continuation for regular optimal control problems*, Optimization Methods and Software, **27** (2011), no. 2, 177–196.

[12] J.-B. Caillau & B. Daoud, *Minimum time control of the restricted three-body problem*, SIAM J. Control Optim., **50** (2012), no. 6, 3178–3202.

[13] E. Hairer, S. P. Nørsett & G. Wanner, *Solving Ordinary Differential Equations I, Nonstiff Problems*, vol 8 of *Springer Serie in Computational Mathematics*, Springer-Verlag, second edn (1993).

[14] E. Hairer & G. Wanner, *Solving Ordinary Differential Equations II, Stiff and Differential-Algebraic Problems*, vol 14 of *Springer Serie in Computational Mathematics*, Springer-Verlag, second edn (1996).

[15] R. F. Hartl, S. P. Sethi & R. G. Vickson, *A survey of the maximum principles for optimal control problems with state constraints*, SIAM Rev., **37** (1995), no. 2, 181–218.

[16] L. Hascoët & V. Pascual, *The Tapenade Automatic Differentiation tool: principles, model, and specification*, Rapport de recherche RR-7957, INRIA (2012).

[17] D. H. Jacobson, M. M. Lele & J. L. Speyer, *New Necessary Conditions of Optimality for Control Problems with State-Variable Inequality Constraints*, J. Math. Anal. Appl., **35** (1971), 255–284.

[18] J. Gergaud & T. Haberkorn, *Homotopy Method for minimum consumption orbit transfer problem*, ESAIM Control Optim. Calc. Var., **12** (2006), no 2, 294–310.

[19] B. De Jager, T. Van Keulen & J. Kessels, *Optimal Control of Hybrid Vehicles*, in *Advances in Industrial Control*, Springer-Verlag, (2013).

[20] S. Jan, *Minimizing the fuel consumption of a vehicle from the Shell Eco-marathon: a numerical study*, ESAIM Control Optim. Calc. Var., **19** (2013), no 2, 516–532.

[21] C. Kirches, H. Bock, J. Schlöder & S. Sager, *Mixed-integer NMPC for predictive cruise control of heavy-duty trucks*, In European Control Conference, pp. 4118–4123. Zurich, Switzerland (2013).

[22] I. Kupka. *Geometric theory of extremals in optimal control problems. i. the fold and maxwell case*, Trans. Amer. Math. Soc., **299** (1987), no. 1, 225–243.

[23] H. Maurer, *On optimal control problems with bounded state variables and control appearing linearly*, SIAM J. Control Optim., **15** (1971), no. 3, 345–362.

[24] A. Merakeb, F. Messine & M. Aidène, *A Branch and Bound algorithm for minimizing the energy consumption of an electrical vehicle* 4OR, **12** (2014), no. 3, 261–283.

[25] J. J. Moré, B. S. Garbow & K. E. Hillstrom, *User Guide for MINPACK-1*, ANL-80-74, Argonne National Laboratory, (1980).

[26] S. Sager, M. Claeys & F. Messine, *Efficient upper and lower bounds for global mixed-integer optimal control* Journal of Global Optimization, **61** (2015), no. 4, 721–743.

[27] H. Schättler & , U. Ledzewicz, *Geometric optimal control: theory, methods and examples*, vol **38** of *Interdisciplinary applied mathematics*, Springer Science & Business Media, New York (2012), xiv+640.

[28] A. Sciarretta & L. Guzzella, *Control of hybrid electric vehicles*, IEEE Control Syst. Mag., **27** (2007), no. 2, 60–70.

The author is thankful to Bernard Bonnard, Jean-Baptiste Caillau and Joseph Gergaud for their geometric and numerical influences on this work.